Supersymmetric Higgs bosons and beyond

Marcela Carena,[1,2] Kyoungchul Kong,[1,3] Eduardo Pontón,[4] and José Zurita[1,5]

[1]*Theoretical Physics Department, Fermilab, Batavia, Illinois 60510, USA*
[2]*Enrico Fermi Institute, University of Chicago, 5640 Ellis Avenue, Chicago, Illinois 60637, USA*
[3]*Theoretical Physics Department, SLAC, Menlo Park, California 94025, USA*
[4]*Department of Physics, Columbia University, 538 West 120th Street, New York, New York 10027, USA*
[5]*Departamento de Física, Universidad de Buenos Aires, (1428) Pabellón 1 Ciudad Universitaria, Capital Federal, Argentina*

We consider supersymmetric models that include particles beyond the minimal supersymmetric standard model (MSSM) with masses in the TeV range, and that couple significantly to the MSSM Higgs sector. We perform a model-independent analysis of the spectrum and couplings of the MSSM Higgs fields, based on an effective theory of the MSSM degrees of freedom. The *tree-level* mass of the lightest *CP*-even state can easily be above the LEP bound of 114 GeV, thus allowing for a relatively light spectrum of superpartners, restricted only by direct searches. The Higgs spectrum and couplings can be significantly modified compared to the MSSM ones, often allowing for interesting new decay modes. We also observe that the gluon fusion production cross section of the SM-like Higgs can be enhanced with respect to both the standard model and the MSSM.

I. INTRODUCTION

Supersymmetry (SUSY) offers an elegant solution to the hierarchy problem, can explain electroweak symmetry breaking (EWSB) dynamically through renormalization group (RG) running and, if established experimentally, could open a window into the physics associated with length scales much shorter than can be probed directly.

The most studied SUSY extension is the minimal supersymmetric standard model (MSSM). In the Higgs sector, the model incorporates two Higgs doublets, H_u and H_d. After EWSB, 5 physical scalars remain in the spectrum [1]. Assuming no *CP* violation, these can be classified as two neutral *CP*-even scalars (h^0 the lightest, H^0 the heaviest), one neutral *CP*-odd scalar (A^0), and a charged Higgs pair ($H^\pm$). The phenomenology in the Higgs sector is largely determined by the masses of these particles, by a mixing angle α that governs the relation between gauge and mass eigenstates in the *CP*-even sector, and by the ratio of the Higgs vacuum expectation values (VEV's), $\tan\beta = v_u/v_d$. In the MSSM only two of these parameters are independent and are conventionally chosen as m_A and $\tan\beta$. Dependence on other sectors of the theory enters through radiative corrections, most notably in the mass of the lightest *CP*-even scalar, h^0. This scalar is found to be below about 130 GeV [2], and together with the direct bounds imposed by LEP suggests the presence of some degree of fine-tuning in the MSSM.

This has been one motivation to study extensions of the MSSM that can either relax the upper bound on the lightest Higgs mass [3,4], or alter its properties in a way that weakens the LEP bounds [5]. Often the extensions considered aim at addressing theoretical issues such as the

μ problem, i.e. how to link the supersymmetric Higgs mass parameter to the scale of EWSB, which in turn is set by the scale of SUSY breaking in the observable sector. Further theoretical constraints are also often imposed, such as the requirement of perturbativity up to a very high scale, the preservation of gauge coupling unification, or various simplifying assumptions that allow one to more easily constrain the low-energy parameters. However, when exploring the Higgs collider phenomenology, it may be healthy to keep an open mind regarding such theoretical assumptions.

If the constraints on the MSSM are to be relaxed, it is necessary to introduce new degrees of freedom (that interact with the MSSM Higgs sector) at or near the weak scale. It has been observed that even if the new particles in the Higgs sector are slightly heavier than the EW scale, the lightest Higgs boson mass may receive important contributions that can relax the LEP constraints [6] (see also [7] for examples with TeV scale vectorlike matter). The new degrees of freedom may or may not be directly accessible at the LHC, but in either case their presence could potentially be inferred by studying the spectrum and couplings of the lighter states. In particular, the observation of a SM-like Higgs with a mass significantly above 130 GeV, together with the observation of other superpartners, would provide a clear hint that the Higgs sector is more complicated than in the MSSM.

We concentrate on supersymmetric scenarios with particles beyond those in the MSSM, under the assumption that they have order one couplings to the MSSM Higgs sector, and that they are heavier than, but close to, the weak scale. This allows one to perform a model-independent analysis of the properties of the lighter states (i.e. those

of the MSSM) by encoding the effects of the heavy physics via higher-dimension operators. As pointed out in [6],[1] at leading order (LO) in $1/M$ (where M is the scale of the heavy physics) only two new parameters are introduced (corresponding to two operators in the superpotential). Therefore, even if the MSSM extension turned out to include a large number of degrees of freedom, their low-energy effects admit a rather simple parametrization. Furthermore, it was found that the $1/M$ effects can give rather important contributions to the mass of the lightest Higgs state. That the effects of such $1/M$-suppressed operators can be as important as those of the renormalizable terms can be understood by considering the structure of the Higgs quartic couplings. In terms of the general two-Higgs doublet model parametrization of [9] [see Eq. (8)], it is well known that of the seven independent quartic couplings only λ_1, λ_2, λ_3, and λ_4 receive contributions in the MSSM, at tree level. The leading order higher-dimension operators contribute to λ_5, λ_6, and λ_7, so that they lead to qualitatively new effects in the Higgs sector. This is the same underlying reason that loop effects in the MSSM, which turn on all possible quartic couplings, can give sizable effects. Thus, the presence of the heavy physics allows a Higgs spectrum consistent with the LEP bounds, even if the SUSY-breaking terms (in the top-stop sector) are of the order of a couple hundred GeV, thus alleviating the tensions found within the MSSM.

Working still at leading order in $1/M$, one finds not only contributions to the quartic Higgs couplings, but also higher-dimension operators in the Higgs potential. These are essential in bounding the scalar potential from below. It was observed in [10] that taking these operators into account leads to the existence of new vacua that can be studied within the above effective field theory (EFT), and that these vacua have distinct properties. For instance, electroweak symmetry breaking is not necessarily controlled by supersymmetry breaking but, unlike in the MSSM, can occur already in the supersymmetric limit (this possibility was considered in the early days of supersymmetry [11], though not in light of the EFT approach; see also Appendix B of Ref. [12], and more recently [13]). These were dubbed "sEWSB vacua" (or supersymmetric EWSB vacua) in [10]. Typical features of the Higgs physics in the sEWSB vacua are order one $\tan\beta$, a heavy CP-even Higgs (H^0) with SM-like properties, and relatively light charginos and neutralinos.

In this work, we further consider the next order in the $1/M$ expansion. On the one hand these lead to the "first order corrections" to the physics in sEWSB vacua [10].

Second, even in MSSM-like vacua their effects can be phenomenologically relevant. This can again be understood by referring to the quartic couplings $\lambda_{1,2,3,4}$, whose size is set at leading order by the electroweak (EW) gauge couplings squared, and hence are numerically small (the source of the lightness of the SM-like Higgs within the MSSM). The $\mathcal{O}(1/M)$ operators from the superpotential do not contribute to these couplings, and therefore the $\mathcal{O}(1/M^2)$ effects become the leading order contributions from the heavy physics to the corresponding quartic operators in the scalar potential. Furthermore, up to numerical factors, the heavy physics gives a contribution of order v^2/M^2 which is comparable to the MSSM one for $M \sim v/g$, with g an EW gauge coupling and v a Lagrangian parameter of the order of the EW scale.[2] At second order in the $1/M$ expansion several new operators appear. Within a given UV completion, the coefficients of these operators may or may not be related to the coefficients of the leading order operators (depending on the complexity of the MSSM extension). Here we do not impose any correlations, but vary the coefficients of the higher-dimension operators (in the superpotential and Kähler potential) independently. Our purpose is to survey the possible signatures in the Higgs sector, which could suggest the presence of an extended sector that might be more difficult to observe directly (for instance if it consists of SM singlets).

Having developed the relevant formalism, in this paper we start a study of the Higgs collider phenomenology. We contrast the observed features against both the SM and MSSM. For instance, we observe a general enhancement of the gluon fusion production cross section of the SM-like Higgs, which is interesting at hadron colliders. Also noteworthy is the fact that the Higgs spectrum can be altered sufficiently to allow for new decay modes with rather significant branching fractions. Here we comment only on some of the possible signals and defer a more complete study of the Higgs collider phenomenology to [14].

Higher-dimension operators in the SUSY context were considered in [8,15], and a more complete classification was presented in [16], where field redefinitions were used to reduce the number of independent operators. The issue of the stability of the Higgs potential for MSSM-like minima (as opposed to sEWSB minima [10]) was considered in [17], while the implications for fine-tuning in such scenarios were considered in [18,19]. Higher-dimension operators can also have interesting consequences for the dark matter relic density [20,21] as well as for cosmology [22] and EW baryogenesis [23–27].

---

[1]The earlier Ref. [8] also considered in detail the effects of higher-dimension operators on the MSSM Higgs sector in the context of low-scale supersymmetry breaking mediation. They also considered effects similar to those we include below, although they restrict to a study of the renormalizable part of the scalar potential.

[2]Note that sizable effects at order $1/M^2$ do not necessarily signal a breakdown of the $1/M$ expansion. In contrast, large effects at order $1/M^3$ in general signal such a breakdown. We take care to study parameter points where the next order effects are expected to be small by a simple criterion described in Sec. IV B.

This paper is organized as follows. In Sec. II, we define the effective theory to be studied and work out the general expressions for the masses and couplings of the light Higgs degrees of freedom to order $1/M^2$. In Sec. III we give simple analytic formulas in certain limits that allow one to understand the qualitative features of the effective theory. In Sec. IV we present the strategy to be used in the numerical study, to be undertaken in Sec. V. There we comment on a selected number of features. A more complete study of the collider phenomenology will be presented in [14]. We conclude in Sec. VI. In Appendix A, we consider several possible UV completions that illustrate how the higher-dimension operators in the EFT can arise. In Appendixes B, C, and D we comment on custodial symmetry violation, give the chargino/neutralino mass matrices, and collect several Higgs trilinear couplings, respectively.

II. EXTENDED SUPERSYMMETRIC HIGGS SECTORS

We start by setting up the framework. Our point of departure is a generic supersymmetric theory with an extended Higgs sector, but where the degrees of freedom beyond those in the MSSM have masses of order M, assumed to be slightly larger than the EW scale. In this case, a model-independent effective field theory analysis is useful. We further assume that all supersymmetry breaking parameters are of the order of a couple hundred GeV, so that the heavy spectrum is approximately supersymmetric, with masses of order M. In this case, it is useful to write the effective theory in supersymmetric notation, keeping track of supersymmetry breaking effects via a spurion superfield that gets a VEV in its F component (we do not consider D-term breaking here). In this section, we define the effective theory to be studied—which describes explicitly only the MSSM Higgs degrees of freedom—and work out the Higgs spectrum and their couplings.

A. Generalized SUSY Two-Higgs doublet model

The effects of heavy particles on the physical properties of the MSSM Higgs fields can be described by a tower of higher-dimension operators suppressed by powers of M. Our ultimate goal is to study the associated collider phenomenology, and we start by working out the spectrum and couplings of the light states (light compared to M). For the reasons spelled out in the Introduction, we work up to next-to-leading order in the $1/M$ expansion. Next-to-next-to-leading order contributions are expected to be small, provided the $1/M$ expansion converges, a point we address in Sec. IV B.

At leading order in $1/M$, the superpotential reads

$$W = \mu H_u H_d + \frac{\omega_1}{2M}(H_u H_d)^2, \tag{1}$$

where $H_u H_d = H_u^0 H_d^0 - H_u^+ H_d^-$ and ω_1 is a dimensionless parameter that we assume to be of order 1. Soft supersymmetry breaking can be parametrized via a spurion superfield $X = m_s \theta^2$, where m_s sets the scale of SUSY breaking (note that we choose X to be dimensionless). Each operator in the superpotential (or Kähler potential) leads to an associated SUSY-breaking operator through multiplication by the spurion, X. We will assume here that the coefficients of the SUSY-breaking operators are proportional to those of the corresponding supersymmetric terms. Besides the $B\mu$ term, at leading order in $1/M$ one has

$$W_{\text{spurion}} = \alpha_1 \frac{\omega_1}{2M} X (H_u H_d)^2 \tag{2}$$

for a dimensionless parameter α_1, also taken to be of order 1. This term leads directly to a quartic interaction among the Higgs scalar fields.

At order $1/M^2$ there are no operators in the superpotential, but several operators enter through the Kähler potential:

$$K = H_d^\dagger e^{2V} H_d + H_u^\dagger e^{2V} H_u + \Delta K^{\not{c}} + \Delta K^c, \tag{3}$$

where

$$\Delta K^{\not{c}} = \frac{c_1}{2|M|^2}(H_d^\dagger e^{2V} H_d)^2 + \frac{c_2}{2|M|^2}(H_u^\dagger e^{2V} H_u)^2$$
$$+ \frac{c_3}{|M|^2}(H_u^\dagger e^{2V} H_u)(H_d^\dagger e^{2V} H_d), \tag{4}$$

$$\Delta K^c = \frac{c_4}{|M|^2}|H_u H_d|^2 + \left[\frac{c_6}{|M|^2} H_d^\dagger e^{2V} H_d \right.$$
$$\left. + \frac{c_7}{|M|^2} H_u^\dagger e^{2V} H_u \right](H_u H_d) + \text{H.c.} \tag{5}$$

We separated the higher-dimension contributions in the Kähler potential into those that violate the custodial symmetry, $K^{\not{c}}$, and those that respect it, K^c [see Eqs. (32) and (33), as well as Appendix B].

The above dimension-6 operators lead to associated SUSY-breaking operators as follows:

$$K_{\text{spurion}}^{\not{c}} = \frac{c_1}{|M|^2}[(\gamma_1 X + \gamma_1^* X^\dagger) + \beta_1 X^\dagger X](H_d^\dagger e^{2V} H_d)^2$$
$$+ \frac{c_2}{|M|^2}[(\gamma_2 X + \gamma_2^* X^\dagger) + \beta_2 X^\dagger X](H_u^\dagger e^{2V} H_u)^2$$
$$+ \frac{c_3}{|M|^2}[(\gamma_3 X + \gamma_3^* X^\dagger) + \beta_3 X^\dagger X](H_u^\dagger e^{2V} H_u)$$
$$\times (H_d^\dagger e^{2V} H_d), \tag{6}$$

$$K^c_{spurion} = \frac{c_4}{|M|^2}[(\gamma_4 X + \gamma_4^* X^\dagger) + \beta_4 X^\dagger X]|H_u H_d|^2$$

$$+ \left[\frac{c_6}{|M|^2}(\gamma_6 X + \delta_6 X^\dagger + \beta_6 X^\dagger X)H_d^\dagger e^{2V} H_d \right.$$

$$+ \frac{c_7}{|M|^2}(\gamma_7 X + \delta_7 X^\dagger + \beta_7 X^\dagger X)H_u^\dagger e^{2V} H_u \right]$$

$$\times (H_u H_d) + \text{H.c.}$$ (7)

Here we used the fact that operators like $XH_d^\dagger e^{2V}H_d$ or $XH_u^\dagger e^{2V}H_u$ can be set to zero by a superfield redefinition [16]. We did not write explicitly the usual soft breaking masses $m_{H_u}^2$ and $m_{H_d}^2$, which correspond to operators of the form $X^\dagger X H_u^\dagger e^{2V}H_u$ and $X^\dagger X H_d^\dagger e^{2V}H_d$, although such terms are understood. We assumed that each type of soft breaking operator vanishes in the absence of the corresponding SUSY-preserving one, i.e. we define the parameters β_i, γ_i, and δ_i by factoring out the associated c_i. This will be the case if the corresponding statement holds in the UV theory that induces the higher-dimension operators we are considering and is a property of several realistic SUSY-breaking mediation mechanisms (in simple extensions one obtains a strict proportionality, as illustrated in the examples described in Appendix A). Notice also that operators like $X^\dagger(H_u H_d)^2$ or $X^\dagger X(H_u H_d)^2$ in the Kähler potential are equivalent to the superpotential operators of Eqs. (1) and (2), and since we are taking ω_1 and α_1 as free parameters, there is no loss of generality in omitting them from Eq. (7).

It is straightforward to work out the scalar potential that follows from Eqs. (1)–(3), (6), and (7) which, at the renormalizable level, takes the form

$$V_{ren.} = m_u^2 H_u^\dagger H_u + m_d^2 H_d^\dagger H_d - [b H_u H_d + \text{H.c.}]$$

$$+ \tfrac{1}{2}\lambda_1(H_d^\dagger H_d)^2 + \tfrac{1}{2}\lambda_2(H_u^\dagger H_u)^2 + \lambda_3(H_u^\dagger H_u)(H_d^\dagger H_d)$$

$$+ \lambda_4(H_u H_d)(H_u^\dagger H_d^\dagger) + \{\tfrac{1}{2}\lambda_5(H_u H_d)^2$$

$$+ [\lambda_6(H_d^\dagger H_d) + \lambda_7(H_u^\dagger H_u)](H_u H_d) + \text{H.c.}\},$$ (8)

where we added the soft masses $m_{H_u}^2$, $m_{H_d}^2$, and b, and $m_{u,d}^2 \equiv m_{H_{u,d}}^2 + |\mu|^2$ also include the supersymmetric mass term, $|\mu|^2$. The quartic operators are defined in such a way that the λ_i, $i = 1, \ldots, 7$, map exactly to those used in [9] with their alternate convention for the hypercharges of the two Higgs-doublet fields. In the MSSM limit, the quartic couplings are

$$\lambda_1^{(0)} = \lambda_2^{(0)} = \frac{1}{4}(g^2 + g'^2), \qquad \lambda_3^{(0)} = \frac{1}{4}(g^2 - g'^2),$$

$$\lambda_4^{(0)} = -\frac{g^2}{2},$$ (9)

with the rest vanishing. At order $1/M$ (henceforth referred to as dimension 5), only λ_5, λ_6, and λ_7 receive contributions:

$$\Delta\lambda_5^{(5)} = -\alpha_1\omega_1\frac{m_s}{M}, \qquad \Delta\lambda_6^{(5)} = \Delta\lambda_7^{(5)} = \omega_1\frac{\mu}{M}.$$ (10)

At order $1/M^2$ all the quartic couplings receive contributions:

$$\Delta\lambda_1^{(6)} = -2(c_3 + c_4)\frac{\mu^2}{M^2} + 4c_6\delta_6\frac{m_s\mu}{M^2} - 2c_1\beta_1\frac{m_s^2}{M^2},$$

$$\Delta\lambda_2^{(6)} = -2(c_3 + c_4)\frac{\mu^2}{M^2} + 4c_7\delta_7\frac{m_s\mu}{M^2} - 2c_2\beta_2\frac{m_s^2}{M^2},$$

$$\Delta\lambda_3^{(6)} = -(c_1 + c_2 + 2c_4)\frac{\mu^2}{M^2} + 2(c_6\delta_6 + c_7\delta_7)\frac{m_s\mu}{M^2} - c_3\beta_3\frac{m_s^2}{M^2},$$

$$\Delta\lambda_4^{(6)} = -(c_1 + c_2 + 2c_3)\frac{\mu^2}{M^2} + 2(c_6\delta_6 + c_7\delta_7)\frac{m_s\mu}{M^2} - c_4\beta_4\frac{m_s^2}{M^2},$$

$$\Delta\lambda_5^{(6)} = 2(c_6\gamma_6 + c_7\gamma_7)\frac{m_s\mu}{M^2},$$

$$\Delta\lambda_6^{(6)} = -(c_6 + 2c_7)\frac{\mu^2}{M^2} + (2c_1\gamma_1 + c_3\gamma_3 + c_4\gamma_4)\frac{m_s\mu}{M^2} - c_6\beta_6\frac{m_s^2}{M^2},$$

$$\Delta\lambda_7^{(6)} = -(c_7 + 2c_6)\frac{\mu^2}{M^2} + (2c_2\gamma_2 + c_3\gamma_3 + c_4\gamma_4)\frac{m_s\mu}{M^2} - c_7\beta_7\frac{m_s^2}{M^2},$$ (11)

where we assumed, as we will do for simplicity in the rest of the paper, that all parameters are real. At this order we should consider also dimension-6 operators in the scalar potential that give parametrically comparable effects. The dimension-6 operators generated by integrating out the F and D terms take the form

$$V_{nonren.} = \frac{1}{M^2}\{|H_u H_d|^2[(\lambda_8 H_d^\dagger H_d + \lambda_8' H_u^\dagger H_u))] + (\lambda_9|H_u H_d|^2 + \lambda_{10}(H_d^\dagger H_d)^2 + \lambda_{11}(H_u^\dagger H_u)^2$$

$$+ \lambda_{12}(H_d^\dagger H_d)(H_u^\dagger H_u))[H_u H_d + H_u^\dagger H_d^\dagger] + \lambda_{13}(H_d^\dagger H_d)^3 + \lambda_{14}(H_d^\dagger H_d)^2(H_u^\dagger H_u)$$

$$+ \lambda_{15}(H_d^\dagger H_d)(H_u^\dagger H_u)^2 + \lambda_{16}(H_u^\dagger H_u)^3\},$$ (12)

where

$$\lambda_8 = \omega_1^2 - (c_1 + c_3)\frac{g^2}{2}, \qquad \lambda_8' = \omega_1^2 - (c_2 + c_3)\frac{g^2}{2},$$

$$\lambda_9 = -(c_6 + c_7)\frac{g^2}{2}, \qquad \lambda_{10} = c_6\frac{(g^2 + g'^2)}{4},$$

$$\lambda_{11} = c_7\frac{(g^2 + g'^2)}{4}, \qquad \lambda_{12} = (c_6 + c_7)\frac{(g^2 - g'^2)}{4},$$

$$\lambda_{13} = c_1\frac{(g^2 + g'^2)}{4}, \qquad \lambda_{14} = c_3\frac{g^2}{2} - c_1\frac{(g^2 - g'^2)}{4},$$

$$\lambda_{15} = c_3\frac{g^2}{2} - c_2\frac{(g^2 - g'^2)}{4}, \qquad \lambda_{16} = c_2\frac{(g^2 + g'^2)}{4}. \tag{13}$$

The operators with coefficients λ_8 and λ_8' are essential in stabilizing the sEWSB vacua discussed in [10]. At order $1/M^2$, higher-dimension operators involving two derivatives need also to be included, since after EWSB they lead to contributions to the Higgs kinetic terms. After canonical normalization, these give additional contributions to the masses and couplings of the Higgs fields. These operators are found to be

$$\mathcal{L} \supset -\frac{1}{M^2}\{c_1([(D^2 H_d)^\dagger H_d](H_d^\dagger H_d) + [(D_\mu H_d)^\dagger H_d][(D^\mu H_d)^\dagger H_d]) + c_2([(D^2 H_u)^\dagger H_u](H_u^\dagger H_u) + [(D_\mu H_u)^\dagger H_u]$$

$$\times [(D^\mu H_u)^\dagger H_u]) + c_3([(D^2 H_u)^\dagger H_u](H_d^\dagger H_d) + [(D^2 H_d)^\dagger H_d](H_u^\dagger H_u) + 2[(D_\mu H_u)^\dagger H_u][(D^\mu H_d)^\dagger H_d])$$

$$- c_4 \partial_\mu(H_u^\dagger H_d^\dagger)\partial^\mu(H_u H_d) + ([c_6(D^2 H_d)^\dagger H_d + c_7(D^2 H_u)^\dagger H_u](H_u H_d) + \text{H.c.})\}, \tag{14}$$

where $D^2 = D_\mu D^\mu$ and $D_\mu = \partial_\mu + igW_\mu + ig'YB_\mu$ is the gauge covariant derivative ($Y = +1/2$ for H_u and $Y = -1/2$ for H_d).

Finally, although there can be $\mathcal{O}(1/M^2)$ contributions to the gauge kinetic terms, we do not consider them here (but see [8]).

B. Higgs spectrum

We obtain the spectrum and couplings of the Higgs fields in two steps: first we neglect the noncanonical kinetic terms that follow from Eq. (14), minimize the potential (which does not require canonical normalization), and obtain general expressions for the (at this point unphysical) masses and couplings in terms of

$$\lambda_i = \lambda_i^{(0)} + \Delta\lambda_i^{(5)} + \Delta\lambda_i^{(6)} + \Delta\lambda_i^{1\text{-loop}}, \tag{15}$$

where the last term represents the 1-loop corrections (to be included in the numerical analysis of Sec. V), which will be discussed in Sec. IV E. In this section we concentrate on the tree-level contributions [i.e. the first three terms in Eq. (15)]. Second, we make a field redefinition to arrive at canonical normalization in the presence of the operators of Eq. (14), and rediagonalize to obtain the physical spectrum. The first step defines CP eigenstates h^0, H^0, A^0, and $H^\pm$, with mass parameters $m_{h^0}^2$, $m_{H^0}^2$, $m_{A^0}^2$, and $m_{H^\pm}^2$ as follows:

$$\begin{pmatrix} H_u^0 \\ H_d^0 \end{pmatrix} = \frac{1}{\sqrt{2}}\begin{pmatrix} v_u \\ v_d \end{pmatrix} + \frac{1}{\sqrt{2}}\begin{pmatrix} c_\alpha & s_\alpha \\ -s_\alpha & c_\alpha \end{pmatrix}\begin{pmatrix} h^0 \\ H^0 \end{pmatrix}$$

$$+ \frac{i}{\sqrt{2}}\begin{pmatrix} s_\beta & c_\beta \\ -c_\beta & s_\beta \end{pmatrix}\begin{pmatrix} G^0 \\ A^0 \end{pmatrix}, \tag{16}$$

$$\begin{pmatrix} H_u^+ \\ H_d^{-*} \end{pmatrix} = \begin{pmatrix} s_\beta & c_\beta \\ -c_\beta & s_\beta \end{pmatrix}\begin{pmatrix} G^+ \\ H^+ \end{pmatrix}, \tag{17}$$

where $s_\beta = \sin\beta$ and $c_\beta = \cos\beta$ with $t_\beta = v_u/v_d$ and $v^2 = v_u^2 + v_d^2 \approx (246 \text{ GeV})^2$. For small fluctuations, $G^{0,\pm}$ are the eaten Goldstone bosons that will be set to zero in the following. Minimization of the potential requires

$$m_u^2 = bt_\beta^{-1} - \frac{v^2}{2}s_\beta^2[\lambda_2 + 3\lambda_7 t_\beta^{-1} + \tilde\lambda_3 t_\beta^{-2} + \lambda_6 t_\beta^{-3}]$$

$$- \frac{v^4}{4M^2}s_\beta^4[3\lambda_{16} + 5\lambda_{11}t_\beta^{-1} + 2\tilde\lambda_8' t_\beta^{-2} + 3\tilde\lambda_9 t_\beta^{-3}$$

$$+ \tilde\lambda_8 t_\beta^{-4} + \lambda_{10} t_\beta^{-5}], \tag{18}$$

$$m_d^2 = bt_\beta - \frac{v^2}{2}t_\beta s_\beta^2[\lambda_7 + \tilde\lambda_3 t_\beta^{-1} + 3\lambda_6 t_\beta^{-2} + \lambda_1 t_\beta^{-3}]$$

$$- \frac{v^4}{4M^2}t_\beta s_\beta^4[\lambda_{11} + \tilde\lambda_8' t_\beta^{-1} + 3\tilde\lambda_9 t_\beta^{-2} + 2\tilde\lambda_8 t_\beta^{-3}$$

$$+ 5\lambda_{10} t_\beta^{-4} + 3\lambda_{13} t_\beta^{-5}], \tag{19}$$

where $\hat\lambda_3 = \lambda_3 + \lambda_4$, $\tilde\lambda_3 = \hat\lambda_3 + \lambda_5$, $\tilde\lambda_8 = \lambda_8 + \lambda_{14}$, $\tilde\lambda_8' = \lambda_8' + \lambda_{15}$, and $\tilde\lambda_9 = \lambda_9 + \lambda_{12}$. The masses of the CP-odd and charged Higgses, A^0 and $H^\pm$, can then be written as

$$m_{A^0}^2 = \frac{bt_\beta}{s_\beta^2} - \frac{v^2}{2}t_\beta(\lambda_7 + 2\lambda_5 t_\beta^{-1} + \lambda_6 t_\beta^{-2})$$

$$- \frac{v^4}{4M^2}t_\beta s_\beta^2[\lambda_{11} + \tilde\lambda_9 t_\beta^{-2} + \lambda_{10} t_\beta^{-4}], \tag{20}$$

$$m_{H^\pm}^2 = m_{A^0}^2 + \frac{v^2}{2}(\lambda_5 - \lambda_4) - \frac{v^4}{4M^2}s_\beta^2(\lambda_8' + 2\lambda_9 t_\beta^{-1} + \lambda_8 t_\beta^{-2}). \tag{21}$$

The mass matrix for the *CP*-even states in the $(h_d, h_u) = (c_\alpha H^0 - s_\alpha h^0, c_\alpha h^0 + s_\alpha H^0)$ basis is

$$\mathcal{M}^2 = m_{A^0}^2 s_\beta^2 \begin{pmatrix} 1 & -t_\beta^{-1} \\ -t_\beta^{-1} & t_\beta^{-2} \end{pmatrix} + v^2 s_\beta^2 \begin{pmatrix} \lambda_5 + 2\lambda_6 t_\beta^{-1} + \lambda_1 t_\beta^{-2} & \lambda_7 + \hat{\lambda}_3 t_\beta^{-1} + \lambda_6 t_\beta^{-2} \\ \lambda_7 + \hat{\lambda}_3 t_\beta^{-1} + \lambda_6 t_\beta^{-2} & \lambda_2 + 2\lambda_7 t_\beta^{-1} + \lambda_5 t_\beta^{-2} \end{pmatrix} + \frac{v^4 s_\beta^4}{M^2}$$

$$\times \begin{pmatrix} \tilde{\lambda}_9 t_\beta^{-1} + \tilde{\lambda}_8 t_\beta^{-2} + 4\lambda_{10} t_\beta^{-3} + 3\lambda_{13} t_\beta^{-4} & \lambda_{11} + \tilde{\lambda}_8' t_\beta^{-1} + 2\tilde{\lambda}_9 t_\beta^{-2} + \tilde{\lambda}_8 t_\beta^{-3} + \lambda_{10} t_\beta^{-4} \\ \lambda_{11} + \tilde{\lambda}_8' t_\beta^{-1} + 2\tilde{\lambda}_9 t_\beta^{-2} + \tilde{\lambda}_8 t_\beta^{-3} + \lambda_{10} t_\beta^{-4} & 3\lambda_{16} + 4\lambda_{11} t_\beta^{-1} + \tilde{\lambda}_8' t_\beta^{-2} + \tilde{\lambda}_9 t_\beta^{-3} \end{pmatrix}, \tag{22}$$

which leads to mass eigenvalues and a mixing angle α given by

$$m_{H^0, \hat{h}^0}^2 = \tfrac{1}{2}[\text{Tr}\,\mathcal{M}^2 \pm \sqrt{(\text{Tr}\,\mathcal{M}^2)^2 - 4\det\mathcal{M}^2}], \tag{23}$$

$$s_{2\alpha} = \frac{2\mathcal{M}_{12}^2}{\sqrt{(\text{Tr}\,\mathcal{M}^2)^2 - 4\det\mathcal{M}^2}}, \tag{24}$$

$$c_{2\alpha} = \frac{\mathcal{M}_{11}^2 - \mathcal{M}_{22}^2}{\sqrt{(\text{Tr}\,\mathcal{M}^2)^2 - 4\det\mathcal{M}^2}}. \tag{25}$$

In order to find the physical masses at order $1/M^2$ we need to include the operators in Eq. (14) that contribute to the kinetic terms of h^0, H^0, A^0, and $H^\pm$. Canonical normalization is achieved by the field redefinitions

$$h^0 \rightarrow (1 - \tfrac{1}{2}A_1)h^0 - \tfrac{1}{2}B_1 H^0, \qquad A^0 \rightarrow (1 - \tfrac{1}{2}E_1)A^0,$$

$$H^0 \rightarrow (1 - \tfrac{1}{2}D_1)H^0 - \tfrac{1}{2}B_1 h^0, \qquad H^\pm \rightarrow (1 - \tfrac{1}{2}F_1)H^\pm, \tag{26}$$

where

$$A_1 = \frac{v^2}{2M^2}s_\beta^2 \Big\{ c_2(1 + c_{2\alpha}) + c_1 t_\beta^{-2}(1 - c_{2\alpha}) + \frac{1}{2}c_3[s_\beta^{-2} - (1 - t_\beta^{-2})c_{2\alpha} - 2t_\beta^{-1}s_{2\alpha}] + c_4 s_\beta^{-2}c_{\alpha+\beta}^2$$

$$+ c_7[-s_{2\alpha} + 2t_\beta^{-1}(1 + c_{2\alpha})] + c_6 t_\beta^{-1}[2(1 - c_{2\alpha}) - t_\beta^{-1}s_{2\alpha}] \Big\},$$

$$B_1 = \frac{v^2}{2M^2}s_\beta^2 \Big\{ (c_2 - c_1 t_\beta^{-2})s_{2\alpha} - \frac{1}{2}c_3[(1 - t_\beta^{-2})s_{2\alpha} - 2t_\beta^{-1}c_{2\alpha}] + c_4 s_\beta^{-2}c_{\alpha+\beta}s_{\alpha+\beta} + c_7(c_{2\alpha} + 2t_\beta^{-1}s_{2\alpha})$$

$$+ c_6 t_\beta^{-1}(-2s_{2\alpha} + t_\beta^{-1}c_{2\alpha}) \Big\},$$

$$D_1 = \frac{v^2}{2M^2}s_\beta^2 \Big\{ c_2(1 - c_{2\alpha}) + c_1 t_\beta^{-2}(1 + c_{2\alpha}) + \frac{1}{2}c_3[s_\beta^{-2} + (1 - t_\beta^{-2})c_{2\alpha} + 2t_\beta^{-1}s_{2\alpha}] + c_4 s_\beta^{-2}s_{\alpha+\beta}^2$$

$$+ c_7[s_{2\alpha} + 2t_\beta^{-1}(1 - c_{2\alpha})] + c_6 t_\beta^{-1}[2(1 + c_{2\alpha}) + t_\beta^{-1}s_{2\alpha}] \Big\},$$

$$E_1 = \frac{v^2}{2M^2} \Big\{ \frac{1}{8}(c_1 + c_2)[1 - s_\beta^4(1 - 14t_\beta^{-2} + t_\beta^{-4})] + \frac{1}{4}c_3[3 + s_\beta^4(1 + 2t_\beta^{-2} + t_\beta^{-4})] + c_4 + 2t_\beta^{-1}s_\beta^2[c_6(1 + s_\beta^2)$$

$$+ c_7(1 + t_\beta^{-2}s_\beta^2)] \Big\},$$

$$F_1 = \frac{v^2}{M^2}s_\beta^4 \Big[\frac{1}{8}c_3(3s_\beta^{-4} + 1 - 6t_\beta^{-2} + t_\beta^{-4}) + t_\beta^{-1}(c_6 + c_7 t_\beta^{-2}) + \frac{1}{2}(c_1 + c_2)t_\beta^{-2} \Big]. \tag{27}$$

At this point, one needs to perform a further rotation (by an angle γ) in the *CP*-even sector that rediagonalizes the corresponding mass matrix:

$$h^0 \rightarrow c_\gamma h^0 + s_\gamma H^0, \qquad H^0 \rightarrow c_\gamma H^0 - s_\gamma h^0, \tag{28}$$

where, to order $1/M^2$,

$$t_{2\gamma} = -\frac{m_{H^0}^2 + m_{h^0}^2}{m_{H^0}^2(1 - D_1) - m_{h^0}^2(1 - A_1)}B_1. \tag{29}$$

We do not expand the denominator to cover cases where $m_{H^0}^2 \approx m_{h^0}^2$. The physical *CP*-even squared masses are finally given by

$$m_h^2 = m_{h^0}^2(1 - A_1)c_\gamma^2 + m_{H^0}^2(1 - D_1)s_\gamma^2$$

$$+ B_1(m_{H^0}^2 + m_{h^0}^2)c_\gamma s_\gamma,$$

$$m_H^2 = m_{H^0}^2(1 - D_1)c_\gamma^2 + m_{h^0}^2(1 - A_1)s_\gamma^2$$

$$- B_1(m_{H^0}^2 + m_{h^0}^2)c_\gamma s_\gamma, \tag{30}$$

while the physical *CP*-odd and charged Higgs masses are given by $m_{A^0}^2(1 - E_1)$ and $m_{H^\pm}^2(1 - F_1)$, respectively. Whenever $\gamma \ll 1$ we have $m_h^2 \approx m_{h^0}^2(1 - A_1)$ and $m_H^2 \approx m_{H^0}^2(1 - D_1)$. However, there are regions where the denominator in Eq. (29) is small and all orders in γ should be kept, in spite of it formally being of order $1/M^2$.

There is one additional source of corrections at order $1/M^2$ that affect the spectrum, as well as the Higgs couplings to be discussed in the next section. The two-derivative operators in Eq. (14) give contributions to the gauge boson masses as follows:

$$m_Z^2 = \frac{1}{4} g_Z^2 v^2 \left[1 + \frac{v^2}{M^2} s_\beta^4 (c_2 + t_\beta^{-1} c_7 + t_\beta^{-3} c_6 + t_\beta^{-4} c_1) \right],$$
(31)

$$m_W^2 = m_Z^2 c_W^2 (1 + \alpha\tilde{T}),$$
(32)

where

$$\alpha\tilde{T} = -\frac{v^2}{2M^2} s_\beta^4 [c_2 - 2t_\beta^{-2} c_3 + t_\beta^{-4} c_1]$$
(33)

is the contribution from the higher-dimension operators to the Peskin-Takeuchi T parameter. Note that, as mentioned in Sec. II A, only the operators in Eq. (4) contribute to T. At loop level, there are other contributions to the T parameter from the distorted Higgs spectrum (heavier SM-like Higgs in addition to mass splittings among the nonstandard Higgses), as well as from custodially violating mass splittings in the superpartner spectrum [28]. For the time being, we note that by keeping m_Z fixed at the observed value, Eq. (31) implies a shift in v at order $1/M^2$:

$$\frac{\Delta v}{v} \approx -\frac{v^2}{2M^2} s_\beta^4 (c_2 + t_\beta^{-1} c_7 + t_\beta^{-3} c_6 + t_\beta^{-4} c_1), \quad (34)$$

so that the VEV v in this model differs from the SM value of 246 GeV by terms of order $1/M^2$. At this order, only the terms in Eqs. (21) and (22) that are proportional to λ_1, λ_2, λ_3, and λ_4—which are nonvanishing in the MSSM limit—are affected by the shift in the VEV (in particular, m_A^2 is not affected). In practice, at this order in the $1/M$ expansion it is sufficient to use $v = (1 + \Delta v/v) \times 246$ GeV in Eqs. (16)–(30), with $\Delta v/v$ given in Eq. (34).

C. Higgs couplings to fermions and gauge bosons

Here we focus on the couplings of the Higgs scalars to gauge bosons and fermions. Recall that in the MSSM the couplings of the neutral Higgs bosons to fermion pairs, relative to the SM value, $g m_f / 2 m_W$, read (for up-type and down-type quarks)

$$
\begin{array}{lll}
h\bar{t}t: c_\alpha/s_\beta, & H\bar{t}t: s_\alpha/s_\beta, & A\bar{t}t: 1/t_\beta, \\
h\bar{b}b: -s_\alpha/c_\beta, & H\bar{b}b: c_\alpha/c_\beta, & A\bar{b}b: t_\beta,
\end{array}
$$
(35)

while the couplings to a pair of gauge bosons relative to the SM value ($g m_W$ for $V = W$ and $g m_Z/c_W$ for $V = Z$) are

$$hVV: s_{\beta-\alpha}, \qquad HVV: c_{\beta-\alpha}.$$
(36)

These couplings are changed by the higher-dimension operators in two ways: indirectly through the mixing angle α [see Eqs. (22), (24), and (25)], and directly due to the effects associated with the operators of Eq. (14), which include the field redefinitions of Eqs. (26). The latter involve a rescaling and therefore cannot be parametrized as a rotation by an effective angle. These effects correspond to the mixing of the MSSM Higgs fields with heavy degrees of freedom that are not included explicitly in the effective theory, and appear first at order $1/M^2$.

Since it is convenient to give the Higgs couplings relative to the SM values, we need to take into account the shift in the Higgs VEV, Eq. (34), which implies a shift in the Yukawa couplings relative to the SM values: $\Delta y_f/y_f = -\Delta v/v$. Together with the Higgs field redefinition of Eqs. (26) these induce a shift in the Higgs-$\bar{f}f$ couplings at order $1/M^2$ compared to Eqs. (35) (on top of the shifts implicit through the mixing angle α).

Similarly, the normalization of the Higgs-gauge boson couplings to the SM value needs to take into account the shifts in the gauge boson masses given in Eqs. (31) and (32). In addition, the two-derivative operators in Eq. (14) also give direct corrections to these vertices from the terms quadratic in the gauge fields and linear in h^0 or H^0:

$$\frac{g^2 v}{4 c_W^2} (\delta g_{hZZ} h^0 + \delta g_{HZZ} H^0) Z_\mu Z^\mu + \frac{g^2 v}{2} (\delta g_{hWW} h^0$$
$$+ \delta g_{HWW} H^0) W_\mu^+ W^{-\mu},$$

where

$$\delta g_{hZZ} = \frac{v^2}{2M^2} \{ 4 s_\beta^3 (c_2 c_\alpha - c_1 t_\beta^{-3} s_\alpha) + s_\beta^2 [c_7(2c_{\alpha+\beta} + c_{\alpha-\beta}) + c_6 t_\beta^{-2}(2c_{\alpha+\beta} - c_{\alpha-\beta})] \},$$

$$\delta g_{HZZ} = \frac{v^2}{2M^2} \{ 4 s_\beta^3 (c_2 s_\alpha + c_1 t_\beta^{-3} c_\alpha) + s_\beta^2 [c_7(2s_{\alpha+\beta} + s_{\alpha-\beta}) + c_6 t_\beta^{-2}(2s_{\alpha+\beta} - s_{\alpha-\beta})] \},$$

$$\delta g_{hWW} = \frac{v^2}{2M^2} \{ 2 s_\beta^3 (c_2 c_\alpha - c_1 t_\beta^{-3} s_\alpha) + 2 c_3 t_\beta^{-1} s_\beta^2 c_{\alpha+\beta} + s_\beta^2 [c_7(2c_{\alpha+\beta} + c_{\alpha-\beta}) + c_6 t_\beta^{-2}(2c_{\alpha+\beta} - c_{\alpha-\beta})] \},$$

$$\delta g_{HWW} = \frac{v^2}{2M^2} \{ 2 s_\beta^3 (c_2 s_\alpha + c_1 t_\beta^{-3} c_\alpha) + 2 c_3 t_\beta^{-1} s_\beta^2 s_{\alpha+\beta} + s_\beta^2 [c_7(2s_{\alpha+\beta} + s_{\alpha-\beta}) + c_6 t_\beta^{-2}(2s_{\alpha+\beta} - s_{\alpha-\beta})] \}.$$

(37)

These should be combined with the field redefinitions Eqs. (26). Note that the corrections to the Z and W couplings are different only due to the custodially violating coefficients c_1, c_2, and c_3.

Putting all these ingredients together, the couplings of Eqs. (35) and (36) are then generalized as follows. For the light CP-even Higgs, h^0, we get

$$
\begin{aligned}
h\bar{t}t: &\; \frac{1}{s_\beta}\left[c_{\alpha+\gamma}\left(1 - \frac{\Delta v}{v} - \frac{1}{2}A_1\right) - \frac{1}{2}B_1 s_{\alpha-\gamma} + \frac{1}{2}(D_1 - A_1)s_\alpha s_\gamma \right], \\
h\bar{b}b: &\; -\frac{1}{c_\beta}\left[s_{\alpha+\gamma}\left(1 - \frac{\Delta v}{v} - \frac{1}{2}A_1\right) + \frac{1}{2}B_1 c_{\alpha-\gamma} - \frac{1}{2}(D_1 - A_1)c_\alpha s_\gamma \right], \\
hZZ: &\; s_{\beta-\alpha-\gamma}\left(1 + \frac{\Delta v}{v} - \frac{1}{2}A_1\right) - \frac{1}{2}B_1 c_{\beta-\alpha+\gamma} + \frac{1}{2}(D_1 - A_1)c_{\beta-\alpha}s_\gamma + c_\gamma \delta g_{hZZ} - s_\gamma \delta g_{HZZ}, \\
hWW: &\; s_{\beta-\alpha-\gamma}\left(1 + \frac{\Delta v}{v} - \frac{1}{2}\alpha\tilde{T} - \frac{1}{2}A_1\right) - \frac{1}{2}B_1 c_{\beta-\alpha+\gamma} + \frac{1}{2}(D_1 - A_1)c_{\beta-\alpha}s_\gamma + c_\gamma \delta g_{hWW} - s_\gamma \delta g_{HWW},
\end{aligned}
\tag{38}
$$

while for the heavy CP-even Higgs, H^0, we get

$$
\begin{aligned}
H\bar{t}t: &\; \frac{1}{s_\beta}\left[s_{\alpha+\gamma}\left(1 - \frac{\Delta v}{v} - \frac{1}{2}A_1\right) - \frac{1}{2}B_1 c_{\alpha-\gamma} - \frac{1}{2}(D_1 - A_1)s_\alpha c_\gamma \right], \\
H\bar{b}b: &\; \frac{1}{c_\beta}\left[c_{\alpha+\gamma}\left(1 - \frac{\Delta v}{v} - \frac{1}{2}A_1\right) + \frac{1}{2}B_1 s_{\alpha-\gamma} - \frac{1}{2}(D_1 - A_1)c_\alpha c_\gamma \right], \\
HZZ: &\; c_{\beta-\alpha-\gamma}\left(1 + \frac{\Delta v}{v} - \frac{1}{2}A_1\right) - \frac{1}{2}B_1 s_{\beta-\alpha+\gamma} - \frac{1}{2}(D_1 - A_1)c_{\beta-\alpha}c_\gamma + c_\gamma \delta g_{HZZ} + s_\gamma \delta g_{hZZ}, \\
HWW: &\; c_{\beta-\alpha-\gamma}\left(1 + \frac{\Delta v}{v} - \frac{1}{2}\alpha\tilde{T} - \frac{1}{2}A_1\right) - \frac{1}{2}B_1 s_{\beta-\alpha+\gamma} - \frac{1}{2}(D_1 - A_1)c_{\beta-\alpha}c_\gamma + c_\gamma \delta g_{HWW} + s_\gamma \delta g_{hWW},
\end{aligned}
\tag{39}
$$

where α is determined by Eqs. (24) and (25). The couplings to fermion pairs of the CP-odd and charged Higgses, A^0 and $H^\pm$, which are independent of α, are obtained from those in the MSSM by multiplication by $(1 - \Delta v/v - \frac{1}{2}E_1)$ and $(1 - \Delta v/v - \frac{1}{2}F_1)$, respectively. Here γ is defined by Eq. (29), A_1, B_1, D_1, F_1, and E_1 are as defined in Eq. (27), $\Delta v/v$ is given in Eq. (34), $\alpha\tilde{T}$ is given in Eq. (33),[3] and δg_{hVV} and δg_{HVV} are given in Eqs. (37). The hVV and HVV couplings in Eqs. (38) and (39) are given relative to gm_Z/c_W and gm_W, respectively, where m_Z and m_W include the order $1/M^2$ corrections as in Eqs. (31) and (32). The Higgs couplings to fermion pairs are given relative to $gm_f/2m_W$, which is the SM Yukawa coupling.

Trilinear interactions involving one gauge boson and two Higgses are also of great phenomenological relevance and receive corrections from the higher-dimension operators of Eq. (3):

$$
\begin{aligned}
\mathcal{L}_3 \supset &\; -\frac{g}{2c_W} Z^\mu \{ (\eta_{ZHA} H^0 \partial_\mu A^0 - \eta_{ZAH} A^0 \partial_\mu H^0) - (\eta_{ZhA} h^0 \partial_\mu A^0 - \eta_{ZAh} A^0 \partial_\mu h^0) \} \\
&\; -\frac{ig c_{2W}}{2c_W} \eta_{ZH^+H^-} Z^\mu (H^+ \partial_\mu H^- - H^- \partial_\mu H^+) - \frac{ig}{2} W^{+\mu} \{ (\eta_{W^\pm hH^\mp} h^0 \partial_\mu H^- - \eta_{W^\pm H^\mp h} H^- \partial_\mu h^0) \\
&\; - (\eta_{W^\pm HH^\mp} H^0 \partial_\mu H^- - \eta_{W^\pm H^\mp H} H^- \partial_\mu H^0) \} + \text{H.c.} - \frac{g}{2} W^{+\mu} \{ \eta_{W^\pm H^\mp A} H^- \partial_\mu A^0 - \eta_{W^\pm AH^\mp} A^0 \partial_\mu H^- \} + \text{H.c.}
\end{aligned}
\tag{40}
$$

We give the detailed form of the coefficients η_{ZhA}, η_{ZAh}, η_{ZHA}, η_{ZAH}, and $\eta_{ZH^+H^-}$, as well as those for the interactions with a single W, in Appendix D.

---

[3]Equations (38) and (39) are the tree-level expressions. There are loop-level contributions to αT, discussed in Sec. IV D, that have to be added. Since experimentally αT is bound to be small, one can neglect it in hWW and HWW for the phenomenologically allowed points.

III. GENERIC FEATURES

In the previous section we presented the effective theory in the Higgs sector up to $\mathcal{O}(1/M^2)$, where M is the scale of the heavy physics. It is useful to obtain simple analytical expressions that hold at order $1/M$, since these will determine the qualitative features induced by the heavy physics. In this section we perform such an analysis and consider several limiting cases that clarify the generic features of the numerical study to be undertaken in the next section.

We start by considering the masses of the CP-even Higgs states, $m_{h^0}^2$ and $m_{H^0}^2$, as given in Eq. (23) with Eqs. (9) and (10). Formally expanding to leading order in $1/M$ one has

$$m_{h^0,H^0}^2 = (m_{h^0,H^0}^2)^{\text{MSSM}} + (\Delta m_{h^0,H^0}^2)^{\text{Dim-5}} + \cdots, \quad (41)$$

where the well-known MSSM contributions, $(m_{h^0}^2)^{\text{MSSM}}$ and $(m_{H^0}^2)^{\text{MSSM}}$, and the leading order corrections due to the heavy physics, $(\Delta m_{h^0}^2)^{\text{Dim-5}}$ and $(\Delta m_{H^0}^2)^{\text{Dim-5}}$, are given by

$$(m_{h^0,H^0}^2)^{\text{MSSM}} = \frac{1}{2}(m_A^2 + m_Z^2 \mp D),$$

$$(\Delta m_{h^0,H^0}^2)^{\text{Dim-5}} = \frac{1}{2}\omega_1 v^2 \left[2s_{2\beta}\left(\frac{\mu}{M}\right)\left(1 \pm \frac{m_A^2 + m_Z^2}{D}\right) \right.$$
$$\left. - \left(\frac{\alpha_1 m_s}{M}\right)\left(1 \mp \frac{c_{2\beta}^2(m_A^2 - m_Z^2)}{D}\right) \right],$$
$$(42)$$

provided one has the inequality

$$D^2 > \omega_1 v^2 \left[2s_{2\beta}\left(\frac{\mu}{M}\right)(m_A^2 + m_Z^2) \right.$$
$$\left. + c_{2\beta}^2\left(\frac{\alpha_1 m_s}{M}\right)(m_A^2 - m_Z^2) \right],$$
$$D \equiv \sqrt{(m_A^2 + m_Z^2)^2 - 4c_{2\beta}^2 m_A^2 m_Z^2}. \quad (43)$$

For the opposite inequality, the expressions for $m_{h^0}^2$ and $m_{H^0}^2$ in Eq. (42) should be interchanged. For typical values of the parameters we are interested in, the inequality Eq. (43) is generally obtained for large m_A, while the opposite inequality results for small m_A. Near the point where the two sides of (43) coincide, the formal expansion to order $1/M$ can be rather inaccurate due to the near degeneracy of the two states (the mixing angle α can receive large corrections). Nevertheless the explicit expressions in Eq. (42) are useful, for instance showing how the sign of the correction to the MSSM result depends on the signs of $\omega_1\mu$ and $\omega_1\alpha_1$.

It is interesting to consider the t_β dependence of the correction to $m_{h^0}^2$ and $m_{H^0}^2$. In the following we assume that the inequality Eq. (43) holds. As discussed above, the complementary region can be obtained by simply interchanging h^0 and H^0 in the relevant statements below. For t_β of order 1 ($s_{2\beta} \approx 1$, $c_{2\beta} \approx 0$), one has

$$(\Delta m_{h^0}^2)^{\text{Dim-5}} \approx \frac{1}{2}\omega_1 v^2\left(\frac{4\mu - \alpha_1 m_s}{M}\right), \quad (44)$$

while for large t_β (i.e. $s_{2\beta} \approx 0$, $|c_{2\beta}| \approx 1$) one has

$$(\Delta m_{h^0}^2)^{\text{Dim-5}} \approx \begin{cases} 0 & m_A \geq m_Z, \\ -\omega_1 v^2(\frac{\alpha_1 m_s}{M}) & m_A < m_Z. \end{cases} \quad (45)$$

Thus, the corrections are most important in the small t_β

regime (if $m_A \gtrsim m_Z$), and this region will allow one to more easily evade the LEP bound on m_{h^0}. This is a well-appreciated feature in models extended by singlet fields, such as the NMSSM and its relatives. We can easily estimate how large m_{h^0} can be for $t_\beta \approx 1$, where the MSSM contribution vanishes. Setting $\alpha_1 \sim -1$ and $\mu \sim m_s$, we have

$$m_{h^0} \sim \sqrt{\omega_1}\frac{v}{\sqrt{2}} \times \mathcal{O}(5\mu/M)^{1/2}. \quad (46)$$

For $\omega_1 \sim 1$ this can easily be above the LEP bound. For the case of large t_β the dimension-6 corrections can play a crucial role in lifting the lightest Higgs mass from the MSSM limit, as will be illustrated in the numerical analysis of the next section (notice that dominant dimension-6 effects do not signal a breakdown of the EFT analysis if the dimension-5 contributions are small due to a t_β suppression or an accidentally small coupling ω_1).

It is also interesting to consider the decoupling limit. Expanding in powers of m_Z^2/m_A^2, one gets

$$(\Delta m_{h^0}^2)^{\text{Dim-5}} \approx \frac{1}{2}\omega_1 v^2 s_{2\beta}\left(\frac{4\mu - s_{2\beta}\alpha_1 m_s}{M}\right), \quad (47)$$

which shows that in a large region of parameter space the leading order correction to m_{h^0} is only suppressed by about $s_{2\beta}$ compared to Eq. (46) [in general, this correction has to be added in quadrature to the MSSM result, according to Eq. (41)].

In Fig. 1 we show the maximum tree-level value of the lightest Higgs mass m_h as a function of m_A, for small $\tan\beta$, fixed representative values of the dimensionful parameters, and assuming that all dimensionless parameters take values at most equal to 1 in absolute value. We show the tree-level value of m_h up to order $1/M$, which is obtained for $\omega_1 = -\alpha_1$ (dash-dotted curve). We also show the maximal values of m_h up to $1/M^2$ effects (dashed curve), and the MSSM (solid) curve for comparison. We see that the effects of the higher-dimension operators can be quite substantial. We emphasize that the effects of order $1/M^3$ or higher are expected to be much smaller, as mentioned in the Introduction and discussed in Sec. IV B.

For the heavy CP-even state we find that $(\Delta m_{H^0}^2)^{\text{Dim-5}} \approx -\frac{1}{2}\omega_1 v^2\alpha_1 m_s/M$ for $\tan\beta \approx 1$. For $\tan\beta \gg 1$, $(\Delta m_{H^0}^2)^{\text{Dim-5}} \approx -\omega_1 v^2\alpha_1 m_s/M$ if $m_A \gtrsim m_Z$, and $(\Delta m_{H^0}^2)^{\text{Dim-5}} \approx 0$ if $m_A < m_Z$. In the decoupling limit $m_A^2 \gg m_Z^2$, we get

$$(\Delta m_{H^0}^2)^{\text{Dim-5}} = -\frac{1}{4}\omega_1 v^2[3 + \cos(4\beta)]\left(\frac{\alpha_1 m_s}{M}\right). \quad (48)$$

Hence, the heavy CP-even state receives corrections at the leading order in the $1/M$ expansion only due to the SUSY-breaking operator, Eq. (2).
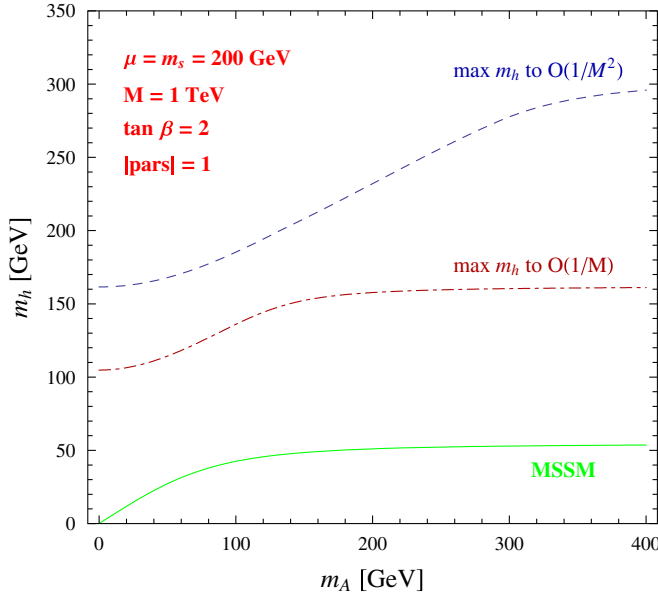
FIG. 1 (color online).   Lightest *CP*-even Higgs tree-level mass, m_h, as a function of m_A, for $\tan\beta = 2$. The dashed blue line corresponds to the maximum value of m_h to $\mathcal{O}(1/M^2)$ when the dimensionless coefficients of the higher-dimension operators are allowed to be as large as 1 (in absolute magnitude). The dash-dotted red line corresponds to the maximum value of m_h to $\mathcal{O}(1/M)$ under the same assumption. The solid green line corresponds to the tree-level MSSM result.

Similarly, the charged Higgs mass takes the form

$$m_{H^\pm}^2 = m_W^2 + m_A^2 - \frac{1}{2}\omega_1 v^2\left(\frac{\alpha_1 m_s}{M}\right), \qquad (49)$$

and, at leading order in $1/M$, gets corrections only from the SUSY-breaking operator, Eq. (2).

Lastly, we consider the corrections to the Higgs couplings at leading order in $1/M$. We start from the mixing angle α which, at this order, is given by

$$t_{2\alpha} = t_{2\beta}\left(\frac{m_A^2 + m_Z^2}{m_A^2 - m_Z^2}\right)$$
$$+ \frac{\omega_1 v^2(-2\mu(m_A^2 - m_Z^2) + s_{2\beta}(m_A^2 + m_Z^2)\alpha_1 m_s)}{Mc_{2\beta}(m_A^2 - m_Z^2)^2}.$$
$$(50)$$

In the decoupling limit this simplifies to

$$t_{2\alpha} = t_{2\beta} + 2t_{2\beta}x + \frac{\omega_1 v^2}{m_A^2 c_{2\beta}}\frac{1}{M}[-2\mu + s_{2\beta}\alpha_1 m_s], \quad (51)$$

where $x = m_Z^2/m_A^2$. Taking into account that α is in the fourth quadrant, while β belongs to the first one, one gets

$$\alpha = \beta - \frac{\pi}{2} + s_{2\beta}c_{2\beta}x + \frac{\omega_1 v^2}{2m_A^2}\frac{c_{2\beta}}{M}[-2\mu + s_{2\beta}\alpha_1 m_s]$$

$$\equiv \beta - \frac{\pi}{2} + A^{(1)}x + A^{(2)}/M. \qquad (52)$$

This implies that the couplings of the *CP*-even Higgs fields to two gauge bosons [see Eqs. (36)] are

$$hVV{:}1 + \mathcal{O}(x^2, v^2/M^2), \qquad HVV{:}A^{(1)}x + A^{(2)}/M. \quad (53)$$

Note that the couplings of the light state to gauge bosons do not receive corrections at order $1/M$ and are not expected to deviate very much from the MSSM ones, while those of the heavy state are expected to get larger corrections. The couplings to fermion pairs relative to the SM are [see Eqs. (35)]

$$h\bar{t}t{:}\ 1 + t_\beta^{-1}(A^{(1)}x + A^{(2)}/M),$$
$$H\bar{t}t{:}\ -t_\beta^{-1}[1 - t_\beta(A^{(1)}x + A^{(2)}/M)],$$
$$h\bar{b}b{:}\ 1 - t_\beta(A^{(1)}x + A^{(2)}/M),$$
$$H\bar{b}b{:}\ -t_\beta[1 + t_\beta^{-1}(A^{(1)}x + A^{(2)}/M)].$$
$$(54)$$

Thus, in the decoupling limit there could be important variations of the light state couplings to the up and down sectors with respect to the SM predictions. However, the $h\bar{t}t$ coupling remains SM like in the large $\tan\beta$ regime. Similarly important variations occur in the couplings of the heavy Higgs to the up-type and down-type fermions, except for the $H\bar{b}b$ coupling in the large $\tan\beta$ regime, where the variations are small.

IV. NUMERICAL ANALYSIS: PARAMETERS AND CONSTRAINTS

In the previous sections we worked out the spectrum and couplings of the Higgs sector in a softly broken super-symmetric theory, under the assumption that there is a set of particles that couple to the MSSM Higgs fields, but that have masses parametrically larger than the weak scale. We also assumed that the SUSY-breaking mass splittings in the heavy supermultiplets are small, so that their masses have a nearly supersymmetric origin. In this section we define the regions or parameter space and discuss several constraints that will be used in the numerical exploration of the effects of the heavy physics on the MSSM Higgs sector, per-formed in Sec. V, and further expanded in [14].

A. Parameter space

We start by defining our region of parameter space. We assume that all SUSY-breaking mass parameters (as well as μ) are of the order of the EW scale (a couple hundred GeV). For definiteness, we take $\mu = m_s = 200$ GeV, where m_s is the F component of the spurion superfield. We also set $M = 1$ TeV. In addition, we scan over the dimensionless parameters defined in Eqs. (1)–(7) as follows:

(i) $|\omega_1|, |c_1|, |c_2|, |c_3|, |c_4|, |c_6|, |c_7| \in [0, 1]$.
(ii) $|\alpha_1|, |\beta_i|, |\gamma_i|, |\delta_i| \in [1/3, 1]$ for $i = 4, 6, 7$.
Recall that the coefficients $\omega_1, c_1, c_2, c_3, c_4, c_6,$ and c_7 set the size of the $1/M$ and $1/M^2$ suppressed operators (both SUSY preserving and SUSY breaking). To be definite we

assume that their values are at most one in absolute magnitude, but it should be clear that if they were larger the physical effects would be correspondingly larger. Our choice for the ranges of $|\alpha_2|$, $|\beta_i|$, $|\gamma_i|$, and $|\delta_i|$ reflects our assumption that the SUSY-breaking operators are proportional to the corresponding SUSY-preserving ones, so that these are parameters of order 1.

We consider two representative values of $\tan\beta$: $\tan\beta = 2$ and $\tan\beta = 20$. We also vary the CP-odd mass up to 400 GeV, which is still below M, ensuring a proper separation between the light and heavy scales, as required by the EFT analysis.

Note that scaling μ, m_s, and M by a common factor leaves the corrections due to the higher-dimension operators, Eqs. (10) and (11), unchanged [though not those of Eqs. (12) and (14)]. In particular, the leading order (dimension-5) operators depend on μ, m_s, and M only through the ratios μ/M and m_s/M. Thus, these effects could be relevant even if the scale of new physics is much higher than we envision here, if SUSY breaking and/or μ are correspondingly larger. Even though we do not scan over the values of μ, m_s, and M (but rather fix them as specified above), our results should be qualitatively applicable when all these scales are higher, keeping the ratios fixed [the difference arises at $\mathcal{O}(1/M^2)$ through the operators of Eqs. (12) and (14)].

B. Uncertainty from higher orders and the EFT expansion

As was mentioned in the Introduction (see also Fig. 1), the contributions of order $1/M$ and $1/M^2$ can be phenomenologically sizable: the $1/M$ effects turn on Higgs quartic couplings not present in the MSSM at tree level, while the $1/M^2$ effects can easily be comparable to the MSSM contribution which is set by the weak gauge couplings. However, one should make sure that the next order can be reasonably expected to give a small contribution, since otherwise it could signal the need to resum the $1/M$ effects to all orders (in which case the details of the UV completion are essential and the EFT approach ceases to be useful). It can also happen (and does happen in our random numerical scans) that there are accidental cancellations between the MSSM contributions proportional to g^2 and those at order $1/M^2$ [see Eq. (11)], or also, if ω_1 is somewhat suppressed, between the order $1/M$ and $1/M^2$ effects. In such cases, the next order corrections can have a larger impact than naively expected, and our $1/M^2$ analysis would fail to capture the quantitative properties of such points in parameter space.

We perform a simple test to assess the robustness of a given point in parameter space against higher-order corrections that have not been computed (and that would depend on new coefficients that are arbitrary from the EFT point of view). Since the most important effects are expected to enter through the Higgs quartic couplings, we

model the next order corrections as follows[4]: keeping all the Lagrangian parameters fixed (m_u^2, m_d^2, b, ω_1, c_i, α_1, γ_i, β_i, δ_6, δ_7, for $i = 1, 2, 3, 4, 6, 7$), we modify the quartic couplings by hand as

$$\lambda_i \rightarrow \lambda_i \pm 2\max\{|\omega_1|, |c_1|, |c_2|, |c_3|, |c_4|, |c_6|, |c_7|\}\left(\frac{\mu}{M}\right)^3,$$
$$i = 1, \ldots, 7, \tag{55}$$

i.e. we allow for $1/M^3$-suppressed operators with dimensionless coefficients as large as those of the leading two orders in the $1/M$ expansion [the factor of 2 models numerical factors that may appear, as we have seen in the order $1/M^2$ expressions, Eqs. (11)]. We then solve the minimization equations, (18) and (19), with these new λ_i's, which leads to values of v and $\tan\beta$ that are slightly different from their values in the absence of the modification. The amount by which these two observables change should give a reasonable measure of the sensitivity of the given parameter point (truncated at order $1/M^2$) to effects from the next order.[5] We restrict ourselves to parameter points for which the above procedure leads to a change of no more than 10% in v. This should be taken as no more than an order of magnitude estimate of the uncertainties associated with the truncation of the tower of higher-dimension operators at order $1/M^2$. We impose a looser constraint on $\tan\beta$: for points with $\tan\beta = 2$, the point is allowed if $1.5 < \tan\beta < 2.5$ after the modification Eq. (55); for points with $\tan\beta = 20$, the point is allowed if $15 < \tan\beta < 25$ after the modification of the λ's. The rationale for a looser constraint in the shift in $\tan\beta$ is that these shifted values would still be representative small and large $\tan\beta$ cases, respectively, and no dramatic change in the Higgs properties is expected within the above ranges.

C. Global versus local minima

The potential given by Eqs. (8) and (12), $V = V_{ren} + V_{nonren.}$, has in general several minima, which may also

---

[4]Notice that at order $1/M^3$ there are only two new operators: the superpotential term $(H_u H_d)^3$ and the associated SUSY-breaking operator. There are no new Kähler operators at this order. However, there are $1/M^3$ effects associated with the lowest order coefficients, e.g. proportional to $\omega_1 c_i$.

[5]Notice that the way to interpret a VEV different from 246 GeV in the presence of the modification Eq. (55) is as follows: one should rescale *all* mass parameters by an appropriate factor so that one recovers the "observed" value for v. This corresponds to normalizing to the measured Z mass and does not change the physics since all mass ratios are kept fixed. Since all mass scales, in particular, the physical Higgs masses, are rescaled by the same factor, we see that the change in the VEV due to the modification Eq. (55) corresponds directly to a change in the spectrum. There can be additional contributions to the spectrum from the higher-dimension operators, not associated with the shift in the VEV, but we expect that these are of the same order as the effect from the shift in the VEV we have described. We therefore consider the above a reasonable estimate of the uncertainties associated with the higher-order operators.

include *CP*-violating or charge breaking VEV's. Without loss of generality, we can parametrize all minima by $\langle H_u \rangle = (0, v_u)$ and $\langle H_d \rangle = (v_d + i v_\delta, v_{CB})$, where v_u, v_d, v_δ, and v_{CB} are real. We can choose this form for $\langle H_u \rangle$ by performing an appropriate $SU(2)_L$ rotation. It is also clear from the fact that the scalar potential depends only on $H_u^\dagger H_u$, $H_d^\dagger H_d$, and $H_u H_d$ that, having set $H_u^+ = 0$, it depends only on $|H_d^-| \equiv v_{CB}$, so we can assume that this latter VEV is real and non-negative. We look numerically for all solutions of the minimizations conditions $\partial_{v_u} V = \partial_{v_d} V = \partial_{v_\delta} V = \partial_{v_{CB}} V = 0$, which are polynomial in the variables, in order to check that the minimum being considered is the global one, and, in particular, preserves charge and *CP*. In this work we do not consider the possibility of explicit nor spontaneous *CP* violation. Also, we do not consider cases where the minimum is metastable but long lived, although such a case can in principle occur and could be phenomenologically viable.

We also recall here the possibility of having different types of (global) minima, as emphasized in [10]. The point is that at the level of quartic couplings, the λ_6 and λ_7 operators in Eq. (8) lead to runaway directions. These are stabilized by dimension-6 operators in the scalar potential, Eq. (12). As a result minima can appear that arise from balancing renormalizable versus nonrenormalizable terms. A simple way to characterize them is to test the scaling $v \propto \sqrt{M}$ in the large *M* limit, keeping all other Lagrangian parameters fixed (see [10] for more details). In contrast, for MSSM-like minima the VEV reaches a finite constant in this limit. We will use this criterion to characterize the type of vacua.

D. Electroweak constraints

Lastly, to assess the viability of a given parameter point, we also estimate the contributions to the oblique parameters in order to select points that are in reasonable agreement with the EW precision constraints. As seen in Eq. (33), the heavy physics can induce tree-level contributions to the Peskin-Takeuchi *T* parameter [29] (see also Appendixes A and B). If one requires $|T| \sim 0.2$ and constrains c_1, c_2, and c_3 one at a time, one sees that for $\tan\beta > 1$ and $M = 1$ TeV, the strongest constraint is $c_2 < 0.1$. Because of the t_β^{-4} and t_β^{-2} suppression in Eq. (33), c_1 and c_3 are less constrained for $\tan\beta > 1$. For instance, if $\tan\beta = 2$ one has $c_1 < 1.3$ and $c_3 < 0.15$ (and are virtually unconstrained for $\tan\beta = 20$). Notice also that there can be partial cancellations in Eq. (33).[6] Thus, even if c_1, c_2, and c_3 are of order 1, provided $M \sim 1$ TeV, these contributions

___

[6]As shown in Appendix A, Higgs triplets give c_1, c_2, $c_3 > 0$. This corresponds to a positive tree-level contribution to *T* from triplets with zero hypercharge and negative from triplets with $Y = \pm 1$. Reference [30] points out that for lighter triplets it is also possible to have a cancellation in *T* arising from the interplay between the triplet mass and the μ term.

to *T* are not necessarily much larger than the experimental limit for a reference Higgs mass of $m_{H_{\text{ref}}} = 117$ GeV.

There are other contributions to *T* that can be comparable to the tree-level one—which is suppressed by v^2/M^2—from loops of the MSSM Higgs fields (SM-like Higgs heavier than $m_{H_{\text{ref}}}$, and mass splittings among the nonstandard Higgses) as well as from custodially violating mass splittings in the (light) superpartner sector. The former give the following contributions to *T* and *S* [31,32]:

$$\alpha T^{\text{Higgs}} \approx \frac{\alpha}{16\pi s_W^2 m_W^2} \{ (\eta_{W^\pm H^\mp A}^{\text{eff}})^2 f(m_{H^\pm}, m_A)$$
$$+ (\eta_{W^\pm H^\mp h}^{\text{eff}})^2 f(m_{H^\pm}, m_h)$$
$$+ (\eta_{W^\pm H^\mp H}^{\text{eff}})^2 f(m_{H^\pm}, m_H) - (\eta_{ZhA}^{\text{eff}})^2 f(m_h, m_A)$$
$$- (\eta_{ZHA}^{\text{eff}})^2 f(m_H, m_A) \} + \Delta\rho_{\text{SM}}(m_h)$$
$$+ \Delta\rho_{\text{SM}}(m_H) - \Delta\rho_{\text{SM}}(m_{H_{\text{ref}}}), \tag{56}$$

$$S^{\text{Higgs}} \approx \frac{1}{12\pi} \{ (\eta_{ZhA}^{\text{eff}})^2 F(m_h, m_A) + (\eta_{ZHA}^{\text{eff}})^2 F(m_H, m_A)$$
$$- (\eta_{ZH^\pm H^\mp}^{\text{eff}})^2 \ln m_{H^\pm}^2 + hZZ^2 \ln m_h^2$$
$$+ HZZ^2 \ln m_H^2 - \frac{5}{6} - \ln m_{H_{\text{ref}}}^2 \}, \tag{57}$$

where α is the fine structure constant, H_{ref} is the reference SM Higgs mass used in the fit to the EW precision measurements, hVV/HVV with $V = Z$, *W* are defined in Eqs. (38), $\eta_{W^\pm H^\mp A}^{\text{eff}} \equiv \frac{1}{2}(\eta_{W^\pm H^\mp A} + \eta_{W^\pm AH^\mp})$, with $\eta_{W^\pm H^\mp A}$, $\eta_{W^\pm AH^\mp}$ as defined in Eqs. (40) (and similar definitions for the other η^{eff}'s), and

$$f(x, y) = \frac{1}{2}(x^2 + y^2) - \frac{x^2 y^2}{x^2 - y^2} \ln\left(\frac{x^2}{y^2}\right),$$

$$\Delta\rho_{\text{SM}}(H_i) = \frac{3\alpha}{16\pi s_W^2 m_W^2} [H_i ZZ^2 f(m_{H_i}, m_Z)$$
$$- H_i WW^2 f(m_{H_i}, M_W)] - \frac{\alpha}{8\pi c_W^2 m_W^2},$$

$$F(m_1, m_2) = \ln(m_1 m_2) + \frac{2m_1^2 m_2^2}{(m_1^2 - m_2^2)^2}$$
$$+ \frac{(m_1^2 + m_2^2)(m_1^4 + m_2^4 - 4m_1^2 m_2^2)}{(m_1^2 - m_2^2)^3} \ln\left(\frac{m_1}{m_2}\right),$$

where $H_i = h, H$. It should be noticed that the expressions (56) and (57) are only approximate since there can be logarithmically divergent terms in the loop computation of the *T* and *S* parameters, in the effective theory with higher-dimension operators, that scale like v^2/M^2 (the quadratically divergent contributions to the gauge boson self-energies vanish by gauge invariance). However, due to the loop suppression, these contributions are expected to be much smaller than the tree-level one, given by Eq. (33),

and are therefore negligible for points where the latter is within the experimental limits (the logarithmic enhancement is small for the scale of new physics we consider).

As remarked in [28] when the SUSY particles are light there can be additional relevant contributions to the T parameter. These depend on parameters that do not affect directly the Higgs sector. As a result, we do not perform here a detailed fit to the EW data. However, we use Eqs. (56) and (57) plus the tree-level contribution, Eq. (33), to estimate whether a given point can be reasonably expected to agree with the precision constraints if appropriate SUSY contributions were added. In Ref. [28] it was found that such SUSY contributions are positive and easily as large as $\Delta T^{\mathrm{SUSY}} \sim 0.2$. Taking $-0.2 < T^{\mathrm{tot}} < 0.3$ (95% C.L.),[7] we therefore allow only points with $-0.4 < \tilde{T} + T^{\mathrm{Higgs}} < 0.3$. After this cut we find that all points in the scan satisfy $-0.05 < S^{\mathrm{Higgs}} < 0.08$, so that we do not impose any further cuts on S.

E. Loop effects

We have implemented our tree-level expressions for the spectrum and Higgs couplings in HDECAY V3.4 [36]. This allows us to also take into account the QCD radiative corrections that are known to be sizable. In addition, we include the radiative corrections derived from the 1-loop RG improved effective potential due to the supersymmetric particles, as computed in [37]. Loop contributions from the heavy physics that has been integrated out are suppressed by both a loop factor and by powers of M; hence they are expected to be negligible.

As we will argue in the next section (see also Fig. 1), already at tree level the Higgs spectrum satisfies the bounds from LEP in large regions of parameter space. Hence, the motivation for taking rather large stop masses is absent in the extensions that we study. Keeping with the philosophy that the SUSY-breaking scale is small compared to M, we consider a relatively light superpartner spectrum. For concreteness we take the superpartner soft parameters to have a common value $M_{\mathrm{SUSY}} = 300$ GeV and $A_t = A_b = 0$.[8] Thus, the SUSY loop contributions to the Higgs masses are modest, but the loop contributions to the Higgs couplings are more important and sensitive to the details of the SUSY spectrum [38,39]. The point to remember is that the relevant loop-level effects can be fully computed given the MSSM superpartner spectrum, and are only mildly dependent on the details of the UV theory that gives rise to the EFT that we study.

---

[7]We use the code of Ref. [33] with $m_t = 173.1 \pm 1.3$ GeV/c^2 [34], $M_W = 80.432 \pm 0.039$ GeV/c^2 [35], and $m_{H_{\mathrm{ref}}} = 117$ GeV.

[8]We denote the soft breaking masses by M_{SUSY}. We evaluate the scale inside the logarithms associated with SUSY loops at $\sqrt{M_{\mathrm{SUSY}}^2 + m_t^2} \approx 347$ GeV.

V. NUMERICAL ANALYSIS: RESULTS

In this section we present the results for the Higgs spectrum and couplings that arise from a scan over the parameter region defined in Sec. IV A. We make sure that we concentrate on parameter points that are expected to be relatively insensitive to higher orders in the $1/M$ expansion, that they correspond to global minima, and that they can be in agreement with the EW precision constraints, given the uncertainties from the SUSY spectrum, as discussed in Secs. IV B, IV C, and IV D. Since our choice of points depends on the "robustness" criterion described in Sec. IV B, we start in Sec. V A by commenting on the consequences of this prescription. We present these results in the *tree-level* approximation, so as to emphasize the effects of the higher-dimension operators.

Next we present the results for some selected observables, such as the gluon fusion production cross section relevant at hadron colliders, and comment on certain "exotic" branching fractions. For these we include the supersymmetric radiative effects to the Higgs masses and couplings, as described in Sec. IV E. We will present a more complete study of the Higgs phenomenology in [14], where we will also include the detailed bounds from LEP and the Tevatron on the Higgs spectrum.

A. Sensitivity against higher-order corrections

We described in Sec. IV B a simple prescription to estimate the sensitivity of a given point in parameter space against $\mathcal{O}(1/M^3)$ effects. In this section we illustrate the dependence on the allowed variation in v by requiring that the VEV change by less than 5%, 10%, and 20% if the next order corrections take a "typical" size, as estimated in Sec. IV B. As an example, we show in Fig. 2 m_h as a function of m_A for $\tan\beta = 2$ (left panel) and $\tan\beta = 20$ (right panel). We have scanned over a total of 10^5 points, but show only those points that correspond to a global minimum and that can be in reasonable agreement with the EW precision constraints, as explained in Sec. IV D. For $\tan\beta = 2$ ($\tan\beta = 20$), we find that about 70% (80%) of the points in the scan correspond to global minima of the potential $V = V_{\mathrm{ren.}} + V_{\mathrm{nonren.}}$, defined by Eqs. (8) and (12), while the rest are only local minima that we discard. The EW precision constraints further reduce the number of potentially viable points in the scan by 70% (80%). In Fig. 2 we exhibit how the number of points is further reduced by requiring $\delta v/v < 0.2$ (green + blue + red regions), $\delta v/v < 0.1$ (green + blue), and $\delta v/v < 0.05$ (green region), following the prescription of Sec. IV B (in the figures we apply the requirements on $\delta \tan\beta$ described in that section). Recall that this gives a measure of the sensitivity of a given point against higher orders in the $1/M$ expansion. The points shown in gray are the additional points that would change by $\delta v/v > 0.2$ under the modification of Eq. (55), and without any restriction on $\delta \tan\beta$
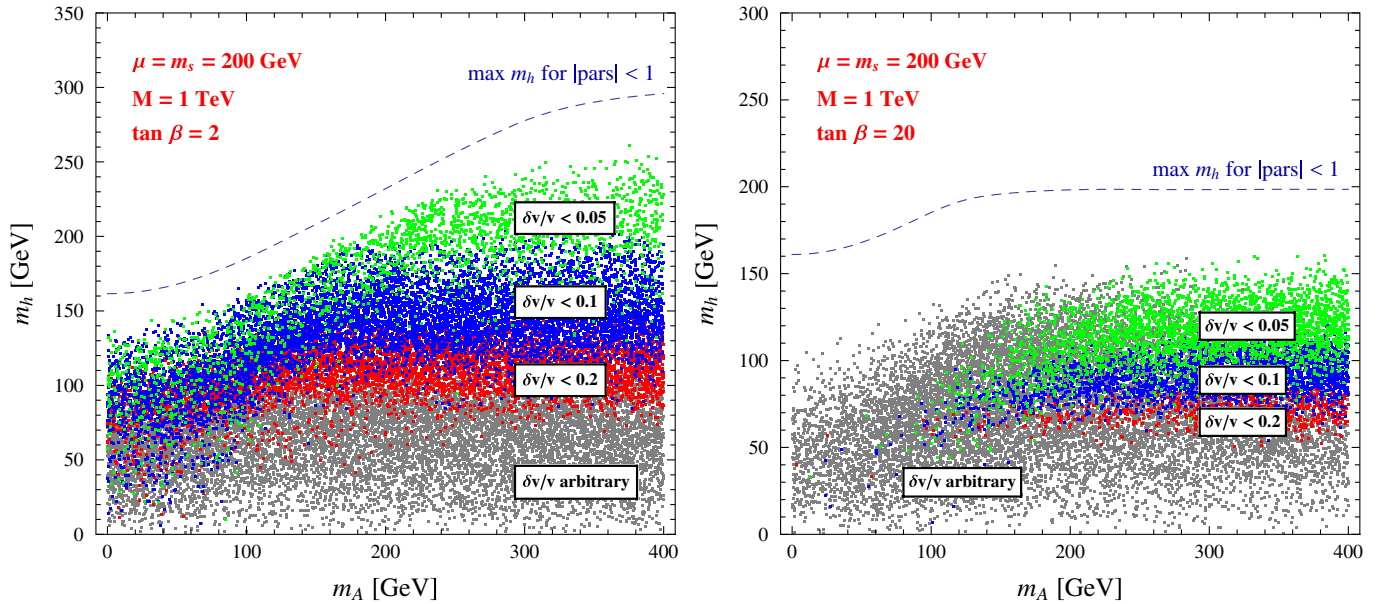
FIG. 2 (color online). Illustration of the sensitivity of m_h against higher-order effects in the $1/M$ expansion, as a function of m_A, for $\tan\beta = 2$ (left panel) and for $\tan\beta = 20$ (right panel). The regions in (green, green + blue, green + blue + red) correspond to the requirement ($\delta v/v < 0.05$, $\delta v/v < 0.1$, $\delta v/v < 0.2$), according to the prescription described in Sec. IV B. The gray points are the additional points in the scan that do not obey any of these three requirements. The dashed blue line corresponds to the maximum tree-level value of m_h when the dimensionless coefficients of the higher-dimension operators are allowed to be as large as 1 (in absolute magnitude). The region of parameter space in the scan is described in the main text.

(i.e. in Fig. 2 we show *all* the points in the scan that are global minima and obey the EW precision constraints).

We observe that the points with smaller m_h are more easily affected by order $1/M^3$ corrections (for instance, they can lead to no EWSB after such a perturbation). This is not to say that there can be no models with small m_h, but only that points where m_h is heavier are relatively insensitive to those higher-order corrections. The reason is that larger m_h indicates that both the $1/M$ and $1/M^2$ effects are contributing fully, without major accidental cancellations (see Sec. IV B). The next order is then suppressed by order v/M, as expected (again, note that all our dimensionless couplings are at most 1). Note also that for $\tan\beta = 20$, the points with small m_A are found to be rather sensitive to the higher-order corrections and tend to be discarded using our prescription. Again, this is not to say that viable models with large $\tan\beta$ and small m_A do not exist, but only that their properties may not be correctly captured at the order we are working, so we choose not to concentrate on such cases. In the following, we restrict to points that satisfy $\delta v/v < 0.1$, which should be interpreted as points for which the higher-order corrections introduce an uncertainty of at most the order of 10%. However, for many points the expected uncertainty should be smaller.

In the figure we also show the maximal value of m_h for the parameter region defined in Sec. IV A. This envelope was obtained by optimizing the values of the dimensionless model parameters so as to maximize m_h. The reason that the points in the scan itself do not reach such large values of m_h is that there is a low probability that *all* the model

parameters simultaneously attain the optimal values that maximize m_h.

B. Higgs masses: Comparison to the MSSM

We start by presenting our results for the Higgs spectrum and comparing it to the MSSM one. We do this at tree-level only. Recall that the radiative corrections are "common" in the MSSM and in the effective theory under study, arising mainly from QCD and the MSSM superpartner sector. The observed differences can therefore be interpreted as arising directly from the heavy physics through the higher-dimension operators. We present in Figs. 3–5 the results of the scan for m_h, m_H, and $m_{H^\pm}$ as a function of m_A, for $\tan\beta = 2$ (left panels) and $\tan\beta = 20$ (right panels). The tree-level MSSM curve is shown for the corresponding m_A and $\tan\beta$. We also indicate which points correspond to sEWSB vacua (red points) and MSSM-like vacua (blue crosses), as described at the end of Sec. IV E. We use the criterion described in [10], which is based on the fact that for large M with all other parameters fixed, the VEV in sEWSB vacua scales like $v \propto \sqrt{M}$. We see that for small $\tan\beta$ a large number of points are of the sEWSB type, while for large $\tan\beta$ most points correspond to MSSM-like vacua.

As expected from our discussion in Sec. III, the corrections to m_h are more important at low $\tan\beta$. However, the scan shows that they can also be relevant at large $\tan\beta$. As already remarked in Sec. V A there are significantly fewer points with small m_h, which is a consequence of the
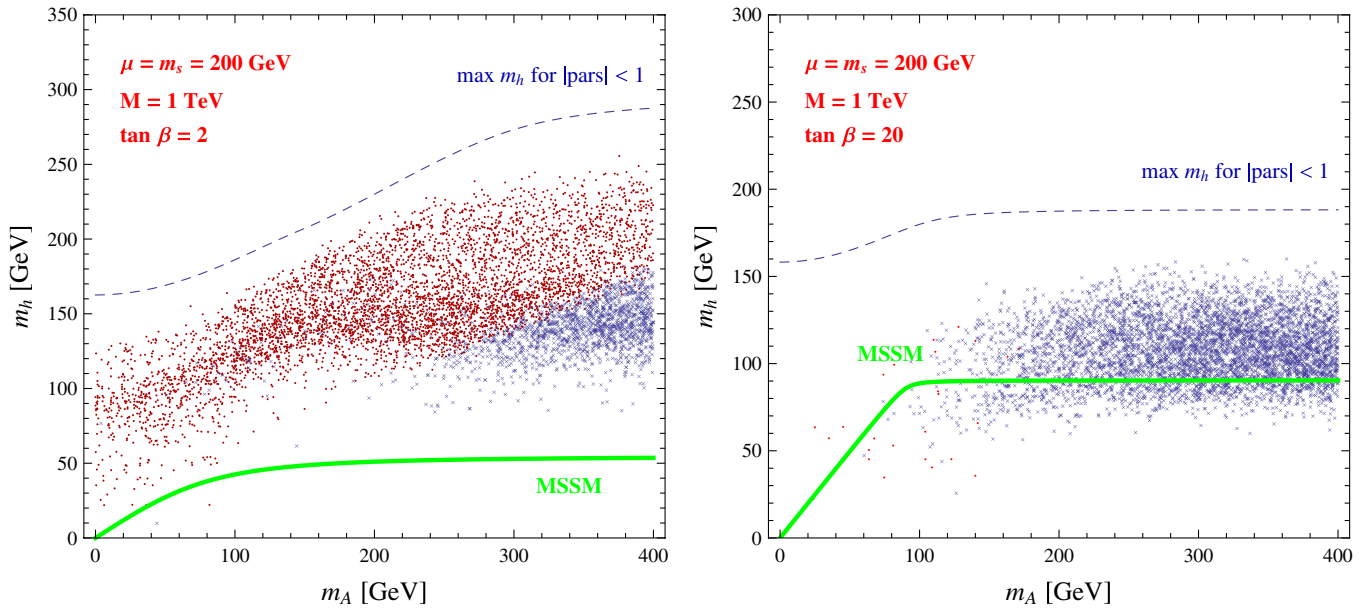
FIG. 3 (color online). Lightest CP-even Higgs tree-level mass, m_h, as a function of m_A, for $\tan\beta = 2$ (left panel) and for $\tan\beta = 20$ (right panel). The dashed blue line corresponds to the maximum value of m_h when the dimensionless coefficients of the higher-dimension operators are allowed to be as large as 1 (in absolute magnitude). The region of parameter space in the scan is described in the main text. The solid green line corresponds to the tree-level MSSM result. Red points correspond to sEWSB vacua, while blue crosses correspond to MSSM-like vacua.

"robustness against higher-order corrections" criterion described in Sec. IV B.

It is also interesting that most points in Fig. 3 present significant deviations from the corresponding MSSM values. Our parameter region includes the case where all higher-dimension operators vanish, and therefore includes the MSSM limit. However, in the scan it is unlikely that

all of them become small simultaneously, which explains why there tends to be more points that exhibit important deviations in m_h with respect to the MSSM. In the large $\tan\beta$ case, the overlap with the MSSM for sufficiently large m_h is possible mainly because many of the operators are $1/\tan\beta$ suppressed, and hence, at large $\tan\beta$ the number of relevant coefficients that contribute
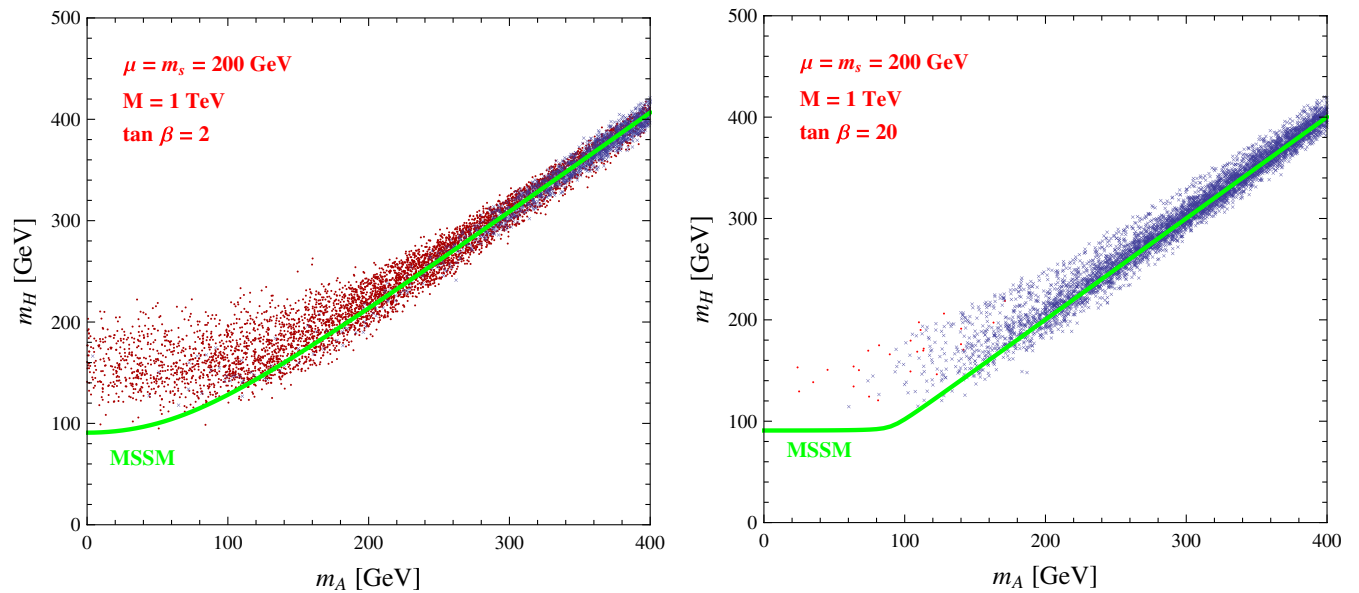

FIG. 4 (color online). Heavy CP-even Higgs tree-level mass, m_H, as a function of m_A, for $\tan\beta = 2$ (left panel) and for $\tan\beta = 20$ (right panel). The solid green line corresponds to the tree-level MSSM result. The region of parameter space in the scan is described in the main text. Red points correspond to sEWSB vacua, while blue crosses correspond to MSSM-like vacua.
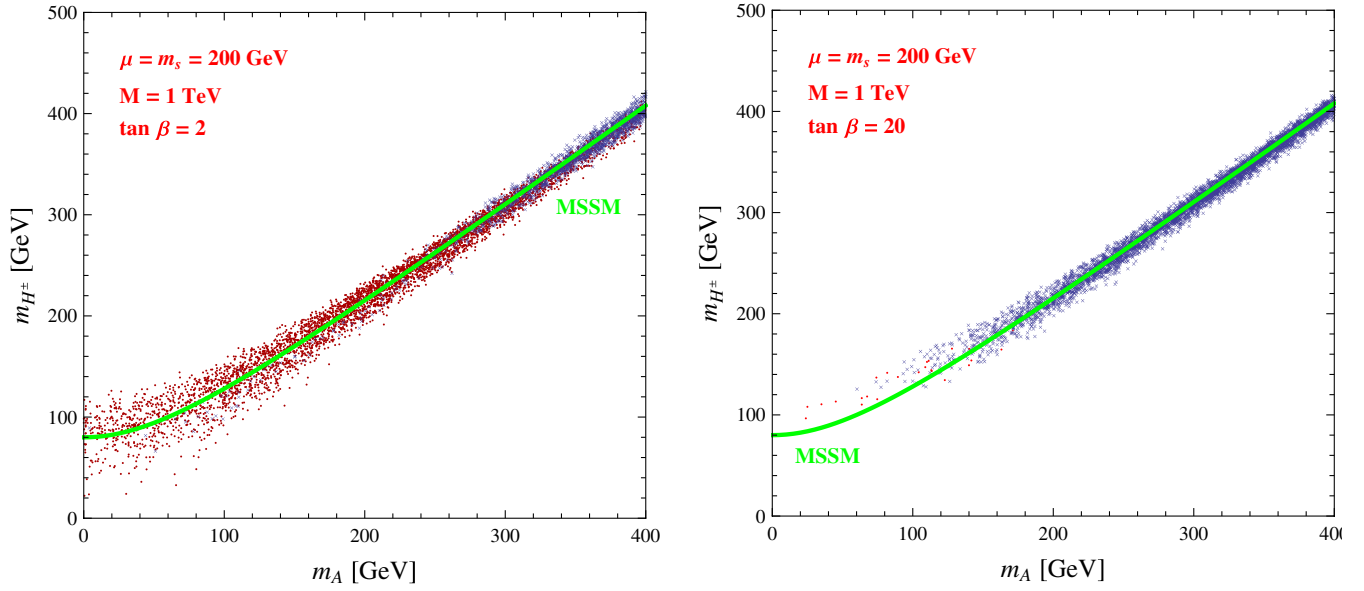
FIG. 5 (color online).   Charged Higgs tree-level mass, $m_{H^{\pm}}$, as a function of m_A, for $\tan\beta = 2$ (left panel) and for $\tan\beta = 20$ (right panel). The solid green line corresponds to the tree-level MSSM result. The region of parameter space in the scan is described in the main text. Red points correspond to sEWSB vacua, while blue crosses correspond to MSSM-like vacua.

to the departure of the Higgs spectrum from the MSSM one is smaller than at low $\tan\beta$. This implies that at large $\tan\beta$ there is a higher probability to effectively turn off all the effects from the higher-dimension operators and reproduce the MSSM values for m_h. Our study simply encapsulates the picture of heavy physics of mass M (= 1 TeV) with couplings of order 1 to the MSSM Higgs sector. For instance, the light *CP*-even Higgs can become sufficiently heavy for the W^+W^- and ZZ channels to be kinematically accessible, thus potentially allowing for a SM search of the light supersymmetric Higgs in the dilepton plus missing energy as well as the four-lepton channels.

Figures 4 and 5 show the H and $H^{\pm}$ spectra as a function of the *CP*-odd Higgs mass for two values of $\tan\beta$, respectively. The deviations in m_H and $m_{H^{\pm}}$ from the MSSM values are less dramatic in the large m_A region, but they can be phenomenologically significant for lower values of m_A. Notice for instance that for $m_A \sim 100$ GeV, m_H can be sufficiently large for the decay $H \rightarrow AA$ to be kinematically open. Similarly, the decay $H^{\pm} \rightarrow W^{\pm}A$ can be open. We will further comment on these decay channels in the next section.

C. Higgs couplings to gauge bosons and fermions

In Fig. 6 we present the tree-level couplings (normalized by the SM values) of the *CP*-even Higgses to Z pairs and up-type and down-type fermions, as a function of m_A. The solid curves show the corresponding MSSM tree-level prediction, making it clear that large deviations from the MSSM can be induced via the higher-dimension operators.

The plots in the upper row of Fig. 6 show the couplings of the *CP*-even Higgses to Z pairs for $\tan\beta = 2$ (left panel)

and $\tan\beta = 20$ (right panel). We will refer to the Higgs state that has the largest coupling to the Z as ''SM like'' (i.e. h is SM like if $|g_{hZZ}| > |g_{HZZ}|$, while H is SM like if $|g_{HZZ}| > |g_{hZZ}|$). Recall that the couplings to WW and ZZ are different as a result of the corrections given in Eq. (37). The difference appears at order $1/M^2$ and is of the order of a few percent when these couplings are sizable (e.g. for the SM-like Higgs). For a non-SM-like Higgs with a very small coupling to W's and Z's, the relative difference between the two can be significant. We also note that in the present scenarios $g^2_{hZZ} + g^2_{HZZ}$ need not add up to 1, reflecting the fact that there are additional (heavy) degrees of freedom that have been integrated out. This effect also arises at order $1/M^2$ and we find that for the chosen parameters it can be as large as 7% (this can be seen more clearly in the large m_A region of the figures).

For large m_A, h becomes SM like to a very good approximation, as in the MSSM. However, we also see that in this limit H can have less suppressed couplings to Z pairs than in the MSSM. These are the properties anticipated in Eq. (53). At low m_A and for $\tan\beta = 2$, we see that H becomes SM like to a better degree of approximation than in the MSSM, while h has more suppressed couplings to Z pairs than in the MSSM. There are also a large number of models with intermediate m_A where both *CP*-even Higgses couple significantly to gauge boson pairs. For $\tan\beta = 20$ the situation is similar in the large m_A region. However, there are very few points at low m_A (see Sec. V A for an explanation).

We also notice several features of the $t\bar{t}h$ and $b\bar{b}h$ ($t\bar{t}H$ and $b\bar{b}H$) couplings, which are relevant for gluon fusion induced processes. We consider first the case of low $\tan\beta$. The $t\bar{t}h$ coupling can present a small enhancement over
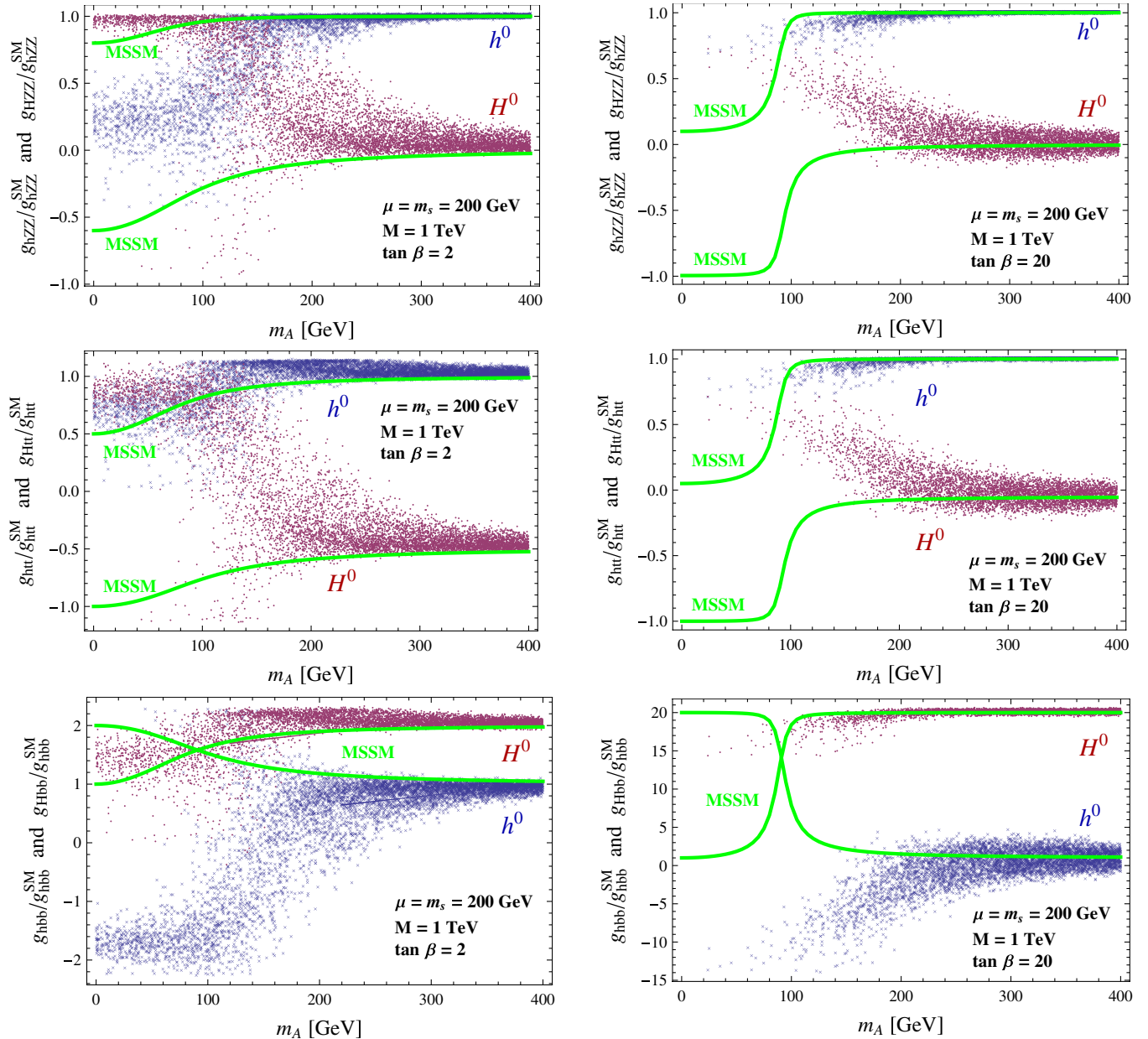
FIG. 6 (color online). Tree-level couplings of the *CP*-even Higgs states (normalized to the SM ones) to gauge bosons (upper plots), to top pairs (middle plots) and to bottom pairs (lower plots), as a function of m_A, for $\tan\beta = 2$ (left panels) and $\tan\beta = 20$ (right panels). The blue crosses correspond to the couplings of h, and the red dots to those of H. The solid green lines correspond to the tree-level MSSM result. The region of parameter space in the scan is described in the main text.

both the SM and the MSSM of up to about 1.2 when $m_A > 100$ GeV (for smaller m_A it can present an enhancement of up to 50% with respect to the MSSM). This would imply a factor of up to 1.4 with respect to the SM prediction for gluon fusion production relevant for searches at the Tevatron and the LHC. In addition, given that there is no need for large radiative corrections to m_h from the squark sector to avoid the bounds on the light Higgs, if a light stop spectrum of the order of a few hundred GeV is present, additional relevant contributions to the gluon fusion process will be expected. These can lead to an additional

enhancement of the reach in gluon fusion induced channels [40]. The $b\bar{b}h$ coupling is suppressed both with respect to the SM and the MSSM when $m_A > 200$ GeV, and reaches a value at most equal to $\tan\beta$ in the low m_A region (as in the MSSM). However, notice that there are a number of models with suppressed couplings to $b\bar{b}$ pairs for $m_A < 140$ GeV.

For low $\tan\beta$ the contribution to gluon fusion is governed by the top Yukawa coupling, and therefore there is a net enhancement with respect to the SM for many models, as seen in the upper left panel of Fig. 7, where we present
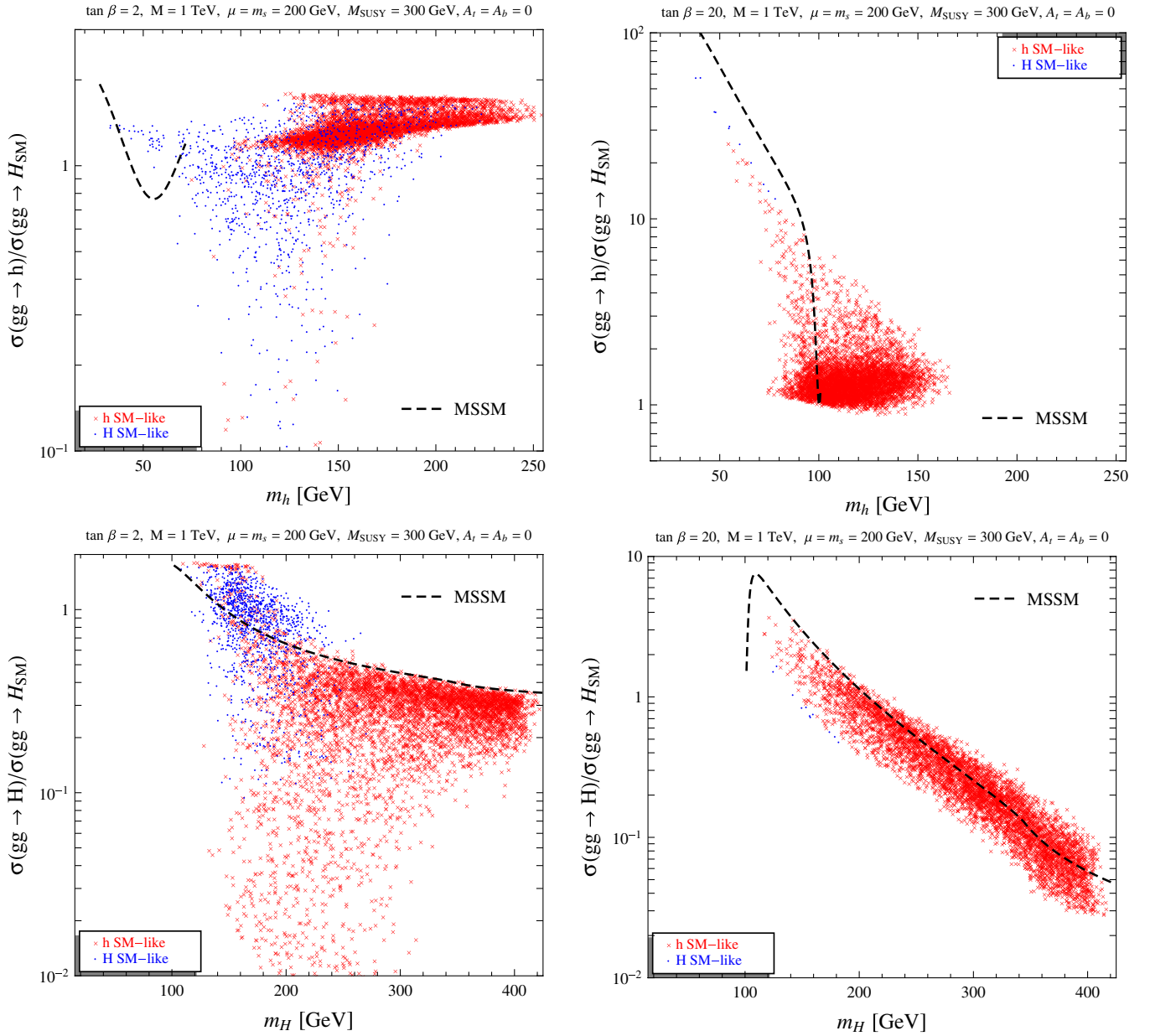
FIG. 7 (color online).   Gluon fusion cross section at LO in α_s, including light SUSY particle loops and normalized to the SM, for the light (upper panels) and heavy (lower panels) *CP*-even Higgses, and for $\tan\beta = 2$ (left panels) and $\tan\beta = 20$ (right panels). The region of parameter space in the scan is described in the main text. We indicate by red crosses those points where h is SM like ($|g_{hZZ}| > |g_{HZZ}|$) and by blue dots those points where H is SM like ($|g_{HZZ}| > |g_{hZZ}|$). The dashed line corresponds to the MSSM result.

the gluon fusion cross section for h production normalized to the SM one, as a function of m_h.[9] In this figure we include the radiative effects to the Higgs masses and couplings assuming a SUSY spectrum as described in

Sec. IV E. Most of the models with $m_h < 115$ GeV are excluded by LEP, while the Tevatron excludes some of the models with m_h in a window around 170 GeV. A detailed analysis of all the cross sections and branching fractions to determine the allowed models will be presented elsewhere [14]. In Fig. 7 we indicate by red crosses the models where h is SM like, as per the definition at the beginning of this section, and by blue dots those models where H is SM like.

The $t\bar{t}H$ coupling at low $\tan\beta$, shown in Fig. 6, is found to be generically suppressed with respect to both the SM

---

[9]We compute $\sigma(gg \to h)/\sigma^{SM}(gg \to h) \approx \Gamma(h \to gg)/\Gamma^{SM}(h \to gg)$, which holds at leading order in α_s [39,41,42]. The values of $\Gamma(h \to gg)$ and $\Gamma^{SM}(h \to gg)$ are calculated at LO using a version of HDECAY [36], modified to include the tree-level expressions in the presence of the higher-dimension operators.

and the MSSM, except for the region $m_A < 200$ GeV where some enhancement may be possible. The $b\bar{b}H$ coupling is generically enhanced with respect to the SM and even with respect to the $\tan\beta$ enhanced value in the MSSM for large m_A. However, the bottom loop contribution to the gluon fusion process is subdominant, as seen in the lower left panel of Fig. 7, where a net suppression with respect to the SM is observed for $m_H > 200$ GeV, governed by the suppression in the $t\bar{t}H$ coupling. In this figure we also see an enhancement with respect to the SM for $m_H < 200$ GeV, which reflects the enhancement of the $t\bar{t}H$ coupling for $m_A < 200$ GeV mentioned above, in addition to the enhancement due to light stop contributions.

At large $\tan\beta$, there is no significant variation in $t\bar{t}h$ with respect to the SM or the MSSM for $m_A > 200$ GeV, but there is a small suppression for 100 GeV $< m_A <$ 200 GeV, and there can be an enhancement with respect to the MSSM for $m_A < 100$ GeV. The $b\bar{b}h$ coupling is enhanced with respect to the SM and the MSSM in a large number of models, and achieves the largest values for $m_A < 100$ GeV, although it is smaller than the $\tan\beta$ value that occurs in the MSSM. For $m_A > 200$ GeV there are many models where the $b\bar{b}h$ coupling is strongly suppressed. As shown in the upper right panel of Fig. 7, in many models the regions of enhanced $b\bar{b}h$ coupling lead to a relevant enhancement of the gluon fusion cross section with respect to the SM one.

At large $\tan\beta$, the $t\bar{t}H$ coupling can have an enhancement with respect to the MSSM in the region 100 GeV $<$ $m_A < 200$ GeV, but is generically suppressed with respect to the SM. The $b\bar{b}H$ coupling presents the familiar $\tan\beta$ enhancement of the MSSM at large m_A, although there could be some suppression in the intermediate region 100 GeV $< m_A < 200$ GeV. At low m_A we see a few models with a significant enhancement of the $b\bar{b}H$ coupling with respect to the SM and the MSSM.

In the large $\tan\beta$ region both top and bottom loops contribute to the gluon fusion cross section with different weights depending on the ratio of the fermion to Higgs masses and the specific (large) value of $\tan\beta$. The lower right panel of Fig. 7 shows that for values of m_H larger than 200 GeV there is always a suppression with respect to the SM gluon fusion cross section for H, similar to the MSSM case.

The couplings of the CP-odd and charged Higgs bosons differ from those of the MSSM only at order $1/M^2$, due to the corrections to their kinetic terms [see comments after Eq. (39)]. These deviations are far less significant than for the CP-even Higgs states. As an example, we show in Fig. 8 the couplings of the CP-odd Higgs to up-type and down-type fermion pairs, which follows closely the $\tan\beta$ enhancement/suppression familiar in the MSSM [see also Eq. (35)].

We postpone a detailed discussion of all the relevant branching fractions and the consequences for Higgs searches at the Tevatron and the LHC to Ref. [14]. Here we comment on a number of selected exotic channels that can motivate new search strategies, in particular, regarding the heavy CP-even and charged Higgs bosons. These are mostly related to the distortion of the Higgs spectrum with respect to the MSSM which can lead to the opening of new decay channels, as mentioned at the end of Sec. V B. For example, we show in the left panel of Fig. 9 the branching fraction for $H \to AA$, which can be significant for m_H up to about 200 GeV. It can be in fact much larger than in the MSSM, where such values of m_H are already near the decoupling limit so that such decays are highly suppressed by phase space. Similarly, there can be important branching fractions for $H \to AZ$, as seen in the right panel of Fig. 9. Note that for most of these points it is H that is SM like.

We also show in the left panel of Fig. 10 that for low $\tan\beta$ there is a generic suppression of the $H \to hh$ channel

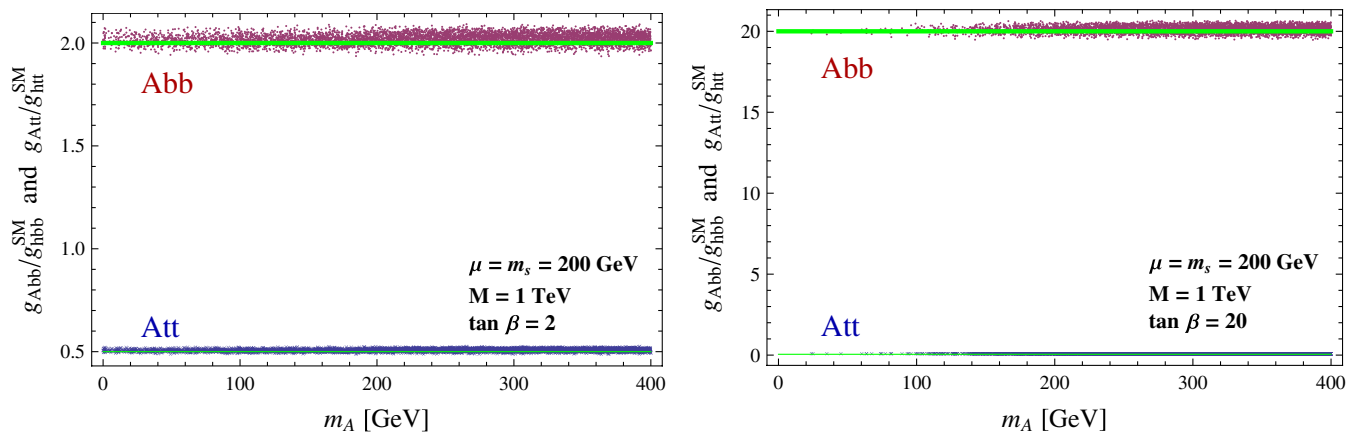

FIG. 8 (color online). Tree-level couplings of the CP-odd Higgs to fermion pairs as a function of m_A, for $\tan\beta = 2$ (left panel) and $\tan\beta = 20$ (right panel), and normalized to the SM value, $g m_f / 2 m_W$. The blue crosses correspond to the couplings of A to $t\bar{t}$, and the red dots to those of A to $b\bar{b}$. The solid green lines correspond to the tree-level MSSM result. The region of parameter space in the scan is described in the main text.
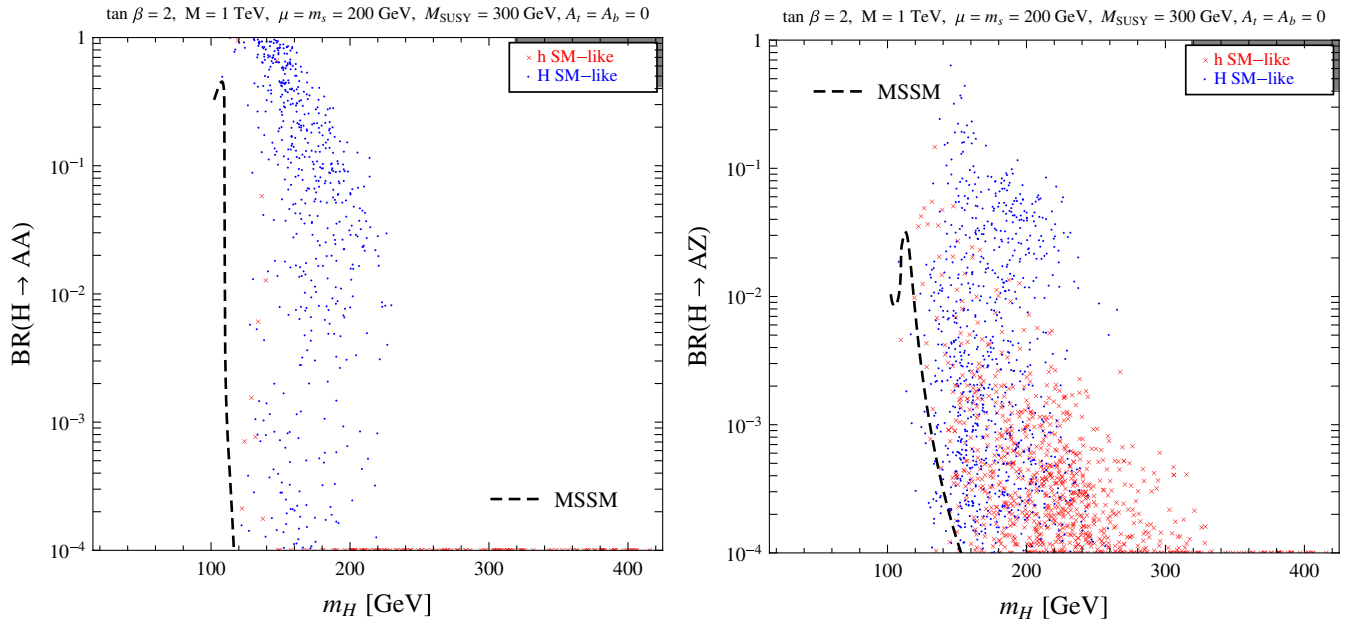
FIG. 9 (color online).   Branching fractions for $H \to AA$ (left panel) and $H \to AZ$ (right panel). The dashed lines correspond to the MSSM results. SUSY and QCD radiative corrections are included. The plots are for $\tan\beta = 2$, $M = 1$ TeV, $\mu = m_s = 200$ GeV, $M_{SUSY} = 300$ GeV, $A_t = A_b = 0$, and a scan over the ranges defined in Sec. IVA. We indicate by red crosses those points where h is SM like ($|g_{hZZ}| > |g_{HZZ}|$) and by blue dots those points where H is SM like ($|g_{HZZ}| > |g_{hZZ}|$).

compared to the MSSM, except above the $t\bar{t}$ threshold where some enhancement is possible (the pronounced dip at $m_H \sim 108$ GeV in the MSSM curve is due to an accidental cancellation of the Hhh coupling; in this small window H decays mostly into b's). The above suppression can be very significant for 170 GeV $< m_H <$ 250 GeV,

reflecting a relatively heavy h so that the channel is closed. At large $\tan\beta$, however, there are large regions where BR($H \to hh$) is enhanced with respect to the MSSM, and in fact $H \to hh$ can be a significant decay channel in this case (see the right panel of Fig. 10).
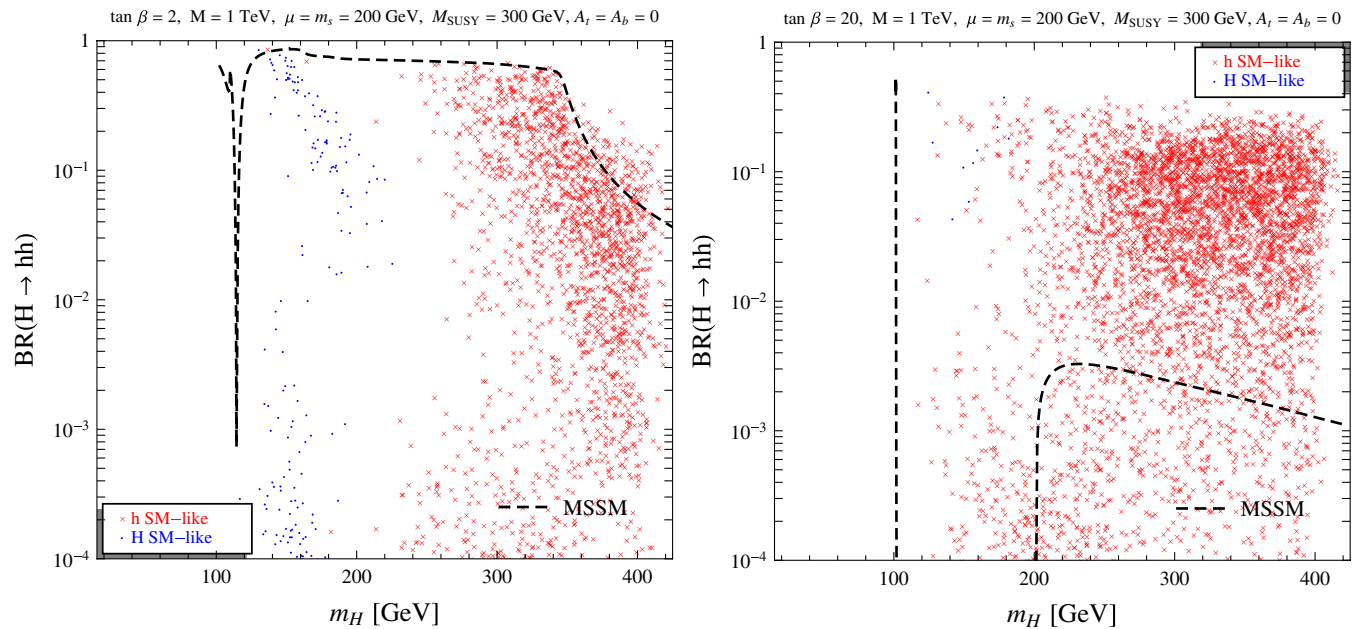

FIG. 10 (color online).   Branching fractions for $H \to hh$ for $\tan\beta = 2$ (left panel) and $\tan\beta = 20$ (right panel). The dashed lines correspond to the MSSM results. SUSY and QCD radiative corrections are included. We indicate by red crosses those points where h is SM like ($|g_{hZZ}| > |g_{HZZ}|$) and by blue dots those points where H is SM like ($|g_{HZZ}| > |g_{hZZ}|$).
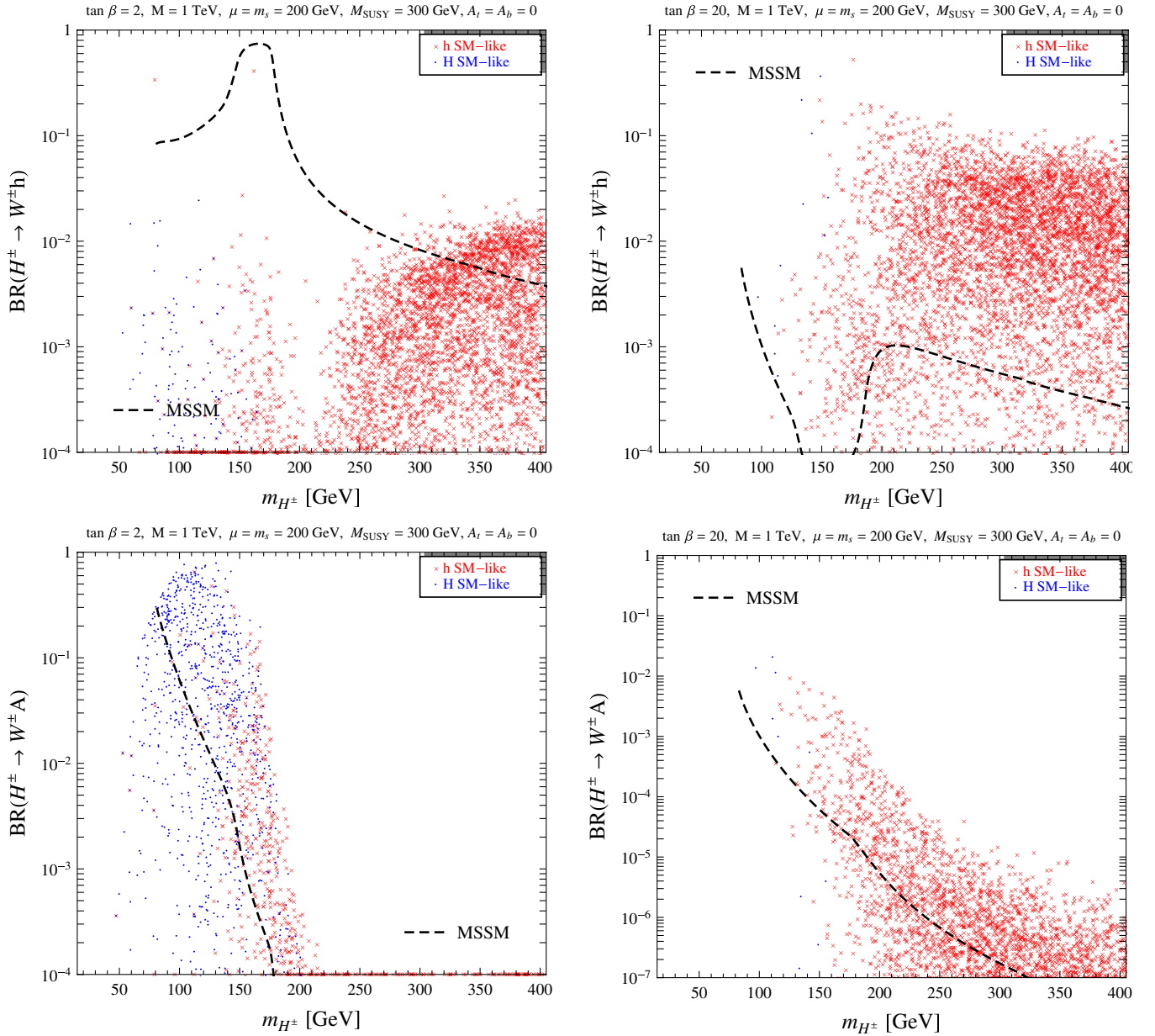
FIG. 11 (color online). Branching fractions for $H^\pm \to W^{\pm(*)}h$ (upper panels) and $H^\pm \to W^{\pm(*)}A$ (lower panels), for $\tan\beta = 2$ (left panels) and $\tan\beta = 20$ (right panels). The dashed lines correspond to the MSSM results. SUSY and QCD radiative corrections are included. We indicate by red crosses those points where h is SM like ($|g_{hZZ}| > |g_{HZZ}|$) and by blue dots those points where H is SM like ($|g_{HZZ}| > |g_{hZZ}|$).

Finally, we comment on certain charged Higgs decays. In the upper row plots of Fig. 11 we present the branching fractions for $H^\pm \to W^\pm h(W^{\pm*}h)$, which show a significant suppression with respect to the MSSM at low $\tan\beta$ (except above the $t\bar{t}$ threshold, where some enhancement is possible), while for large $\tan\beta$ there is an enhancement compared to the MSSM in a large number of models. In the lower row plots of Fig. 11, we see that the branching fraction for $H^\pm \to W^\pm A(W^{\pm*}A)$ can be sizable at low $\tan\beta$ and for $100\ \text{GeV} < m_{H^\pm} < 180\ \text{GeV}$, while it remains small for large $\tan\beta$ (although it can still be en-

hanced compared to the MSSM). Since at low $\tan\beta$, $\text{BR}(H^\pm \to W^\pm A)$ can be close to unity, one may therefore expect to produce a large number of CP-odd Higgs bosons in top decays. Note also that a large fraction of the points with such a property present the "inverted hierarchy" where H is SM like.

VI. CONCLUSIONS

We have considered a large class of supersymmetric scenarios with physics beyond the MSSM that couples

appreciably to the MSSM Higgs sector. Our main assumption is that the degrees of freedom beyond the MSSM are heavier than the weak scale, and that their SUSY mass splittings can be treated as a perturbation. We call this approximately supersymmetric threshold M. As a result, a model-independent analysis can be set up, based on an approximately supersymmetric effective theory of the MSSM that includes higher-dimension operators suppressed by powers of $1/M$. These higher-dimension operators can encapsulate different types of physics beyond the MSSM, such as singlet or triplet Higgses, heavy Z' and W', etc. (we illustrate the detailed connection in Appendix A).

We argued, based on the structure of the induced Higgs quartic couplings, that both the leading and next-to-leading order in the $1/M$ expansion can be phenomenologically relevant, and computed the Higgs spectrum and couplings up to this order. This included a careful treatment of degenerate cases and the inclusion of kinetic term renormalization that contains information about the mixing of the light and heavy degrees of freedom. The most important effects of the new physics enter through the angle α that characterizes the mixing in the CP-even sector, but we have systematically included all the effects to order $1/M^2$. This allows us to include in our analysis the recently discussed sEWSB vacua [10], which depend crucially on certain dimension-6 operators.

We were especially careful to single out points in the effective theory that can be expected to be reliably described by the EFT. We also made sure that these points correspond to global minima of the effective potential (we did not consider the possibility of long-lived metastable minima). In addition, we took into account the EW precision constraints, making sure that the study points can be in agreement with precision tests when possible effects from squarks and sleptons not directly related to the Higgs sector are included.

The large class of SUSY models presented in this study has in part already been explored by various Higgs searches at LEP and the Tevatron. We will present these constraints in the accompanying paper [14]. Similarly, we defer a more complete study of the Higgs collider phenomenology to that work. Here we simply pointed out a few interesting features that arise from our study: a generic enhancement of the gluon fusion production cross section of the SM-like Higgs, the presence of new channels with significant branching fractions, such as $H \rightarrow AA$ and $H^{\pm} \rightarrow W^{\pm}A$, and the possible suppression of decay modes such as $H \rightarrow hh$.

We find it interesting that a study of the light Higgs sector can indirectly reveal the presence of new physics that either may not be within reach, or may not be easy to produce, as was also emphasized recently in [43,44]. The measurement of the Higgs spectrum and observation of some of their decay modes, together with the observation of some of the SM superpartners, can give a striking

evidence for a more complicated structure beyond the MSSM.

ACKNOWLEDGMENTS

APPENDIX A: UV COMPLETIONS

Here we consider possible UV completions to exemplify how the operators of the effective theory can be generated. We consider the addition of singlets, of vectorlike triplets ($Y = \pm 1$), of a triplet with a Majorana mass and $Y = 0$, and an $SU(2)$ gauge extension under which H_u and H_d transform as doublets. This illustrates how the higher-dimension operators on which the EFT analysis presented in the main text is based can arise, and also shows that the coefficients of these operators can be fairly uncorrelated if the extension is sufficiently complicated. This justifies our approach of scanning over these coefficients without taking into account the correlations that may arise in a given UV model.

1. MSSM + singlet

The simplest model we consider shares structural features with the NMSSM. In the NMSSM, a new singlet S is added to the MSSM to solve the μ problem, through a VEV for S and the superpotential interaction $\lambda_S S H_u H_d$. In this model, the low-energy theory contains additional scalar states from S, and after EWSB the singlet state mixes with the Higgs. However, there is a different region of parameter space, where the singlet S has a mass somewhat larger than the electroweak scale and is integrated out of the effective theory. Although the μ problem is not addressed in this limit, the low-energy theory contains modifications in the Higgs sector that can help solve the little SUSY hierarchy problem.

The superpotential and Kähler potential are

$$W = \mu H_u H_d + \tfrac{1}{2} M_S S^2 + \lambda_S S H_u H_d - X(a_1 \mu H_u H_d + \tfrac{1}{2} a_2 M_S S^2 + a_3 \lambda_S S H_u H_d), \tag{A1}$$

$$K = H_u^\dagger e^V H_u + H_d^\dagger e^V H_d + S^\dagger S - X^\dagger X(b_1 H_d^\dagger H_d$$

$$+ b_2 H_u^\dagger H_u + b_3 S^\dagger S), \tag{A2}$$

where the a_i and b_i are dimensionless, and an ϵ tensor is understood in the contraction $H_u H_d \equiv H_u \epsilon H_d$. One can consider a cubic coupling κS^3, but it does not contribute to the effective theory up to the order $1/M^2$ we have analyzed; hence we do not write it explicitly in Eq. (A1). The parameters b_1, b_2, and a_1 map into $m_{H_d}^2$, $m_{H_u}^2$, and the $B\mu$ term, respectively. Integrating out S at tree level induces nonzero ω_1, α_1, c_4, β_4, and γ_4 in Eqs. (1)–(7) as follows:

$$M = M_S, \qquad \omega_1 = -\lambda_S^2,$$

$$\alpha_1 = a_2 - 2a_3, \qquad c_4 = |\lambda_S|^2,$$

$$\gamma_4 = a_2 - a_3, \qquad \beta_4 = |a_2 - a_3|^2 - b_3, \tag{A3}$$

while all other EFT coefficients vanish.

2. MSSM + $SU(2)_L$ Higgs triplets

Consider an extension with two $SU(2)_L$ triplets, T and $\bar{T}$, with hypercharges $Y = -1$ and $Y = +1$, respectively. The superpotential and Kähler potential are

$$W = \mu H_u H_d + M_T T\bar{T} + \tfrac{1}{2}\lambda_T H_u T H_u + \tfrac{1}{2}\lambda_{\bar{T}} H_d \bar{T} H_d$$

$$- X(a_1 \mu H_u H_d + a_2 M_T T\bar{T} + \tfrac{1}{2}a_3 \lambda_T H_u T H_u$$

$$+ \tfrac{1}{2}a_4 \lambda_{\bar{T}} H_d \bar{T} H_d), \tag{A4}$$

$$K = H_d^\dagger e^{2V} H_d + H_u^\dagger e^{2V} H_u + T^\dagger e^{2V} T + \bar{T}^\dagger e^{2V} \bar{T}$$

$$- XX^\dagger(b_1 H_d^\dagger H_d + b_2 H_u^\dagger H_u + b_3 T^\dagger T + b_4 \bar{T}^\dagger \bar{T}). \tag{A5}$$

An epsilon tensor is understood in the contractions $H_u T H_u = H_u \epsilon T H_u$, etc. The parameters b_1, b_2, and a_1 map into $m_{H_d}^2$, $m_{H_u}^2$, and the $b\mu$ term, respectively. Integrating out the triplets, one can write the effective Lagrangian in terms of the operators defined in Eqs. (1)–(7), with[10]

$$M = M_T, \qquad \omega_1 = \tfrac{1}{4}\lambda_T \lambda_{\bar{T}}, \qquad \alpha_1 = a_2 - a_3 - a_4,$$

$$c_1 = \tfrac{1}{4}|\lambda_{\bar{T}}|^2, \qquad \gamma_1 = a_2 - a_4, \qquad \beta_1 = |a_2 - a_4|^2 - b_3,$$

$$c_2 = \tfrac{1}{4}|\lambda_T|^2, \qquad \gamma_2 = a_2 - a_3, \qquad \beta_2 = |a_2 - a_3|^2 - b_4,$$

$$\tag{A6}$$

and all other dimensionless coefficients vanishing.

If on the other hand one considers an extension with a single $SU(2)_L$ triplet with hypercharge $Y = 0$ and a

---

[10]Here we use the identity $\int d^4\theta \mathcal{A}^\dagger e^{2V} \mathcal{A} = \tfrac{1}{2} \times \int d^4\theta (H^\dagger e^{2V} H)^2$, where $\mathcal{A} = \mathcal{A}^a X^a$ with $\mathcal{A}^a = H\epsilon\tau^a H$, and X^a are the $SU(2)$ generators in the adjoint representation while H is in the fundamental representation of $SU(2)$. One also has $\int d^4\theta \mathcal{A}^\dagger e^{2V} \mathcal{A} = \int d^4\theta\{\tfrac{1}{2}(H_u^\dagger e^{2V} H_u)(H_d^\dagger e^{2V} H_d) - \tfrac{1}{4}|H_u \epsilon H_d|^2\}$ for $\mathcal{A}^a = H_u \epsilon\tau^a H_d$.

Majorana mass M_T, the superpotential and Kähler potential are

$$W = \mu H_u H_d + \tfrac{1}{2}M_T T^2 + \lambda_T H_u T H_d$$

$$- X(a_1 \mu H_u H_d + \tfrac{1}{2}a_2 M_T T^2 + a_3 \lambda_T H_u T H_d), \tag{A7}$$

$$K = H_d^\dagger e^{2V} H_d + H_u^\dagger e^{2V} H_u + T^\dagger e^{2V} T$$

$$- XX^\dagger(b_1 H_d^\dagger H_d + b_2 H_u^\dagger H_u + b_3 T^\dagger T), \tag{A8}$$

and after integrating out the triplet, one obtains the effective theory of Eqs. (1)–(7), with

$$M = M_T, \qquad \omega_1 = -\tfrac{1}{4}\lambda_T^2, \qquad \alpha_1 = a_2 - 2a_3,$$

$$c_3 = \tfrac{1}{2}|\lambda_T|^2, \qquad \gamma_3 = a_2 - a_3, \qquad \beta_3 = |a_2 - a_3|^2 - b_3,$$

$$c_4 = -\tfrac{1}{4}|\lambda_T|^2, \qquad \gamma_4 = a_2 - a_3, \qquad \beta_4 = |a_2 - a_3|^2 - b_3,$$

$$\tag{A9}$$

while all other EFT coefficients vanish.

3. $SU(2)$ Extensions

The higher-dimension operators induced by integrating out a massive $U(1)'$ were worked out in Ref. [6]. Here we consider a product gauge group $SU(2)_1 \times SU(2)_2 \times U(1)_Y$ with gauge couplings g_1, g_2, and g', respectively. We concentrate on the $SU(2)_1 \times SU(2)_2$ factor since the $U(1)_Y$ factor enters in a trivial way. The MSSM Higgs superfields are assumed to transform like $(\mathbf{2}, \mathbf{0})$ under $SU(2)_1 \times SU(2)_2$. The gauge group is broken down to the diagonal by a Σ field transforming like $(\mathbf{2}, \mathbf{2})$ under $SU(2)_1 \times SU(2)_2$, which gets a nonzero VEV, $\langle\Sigma\rangle \propto \sigma^2$. In this case, the kinetic term for Σ, $\mathrm{Tr}(e^{2g_2 V_2^T} \Sigma^\dagger e^{2g_1 V_1} \Sigma)$, leads to the structure $\mathrm{Tr}(e^{2g_2 V_2} e^{2g_1 V_1})$, which contains a mass term for the linear combination $V' \equiv (g_1 V_1 + g_2 V_2)/\sqrt{g_1^2 + g_2^2}$. The orthogonal combination $V \equiv (g_2 V_1 - g_1 V_2)/\sqrt{g_1^2 + g_2^2}$ remains massless and can be identified with the SM W gauge bosons. Therefore, we take as the starting point the Kähler potential

$$K = H_u^\dagger e^{2g_1 V_1} H_u + H_d^\dagger e^{2g_1 V_1} H_d$$

$$+ \frac{M_{V'}^2}{2(g_1^2 + g_2^2)} \mathrm{Tr}[e^{2g_2 V_2} e^{2g_1 V_1}], \tag{A10}$$

where $g_1 V_1 = \tilde{g} V' + g V$, $g_2 V_2 = (g_2^2/g_1^2)\tilde{g} V' - g V$, and $g = g_1 g_2/\sqrt{g_1^2 + g_2^2}$ is the SM $SU(2)_L$ gauge coupling while $\tilde{g} = g_1^2/\sqrt{g_1^2 + g_2^2}$ is the coupling of the massive V'. The term of second order in V' in the last term of Eq. (A10) identifies $M_{V'}$ as the gauge boson mass. In order to integrate out V' to order $1/M_{V'}^2$, it is sufficient to keep terms up to quadratic order in V' in the "mass term," while keeping up to linear order in the terms not proportional to $M_{V'}^2$. We can also assume that V is in the Wess-Zumino

gauge so that we can expand to quadratic order in V everywhere. Note that the term proportional to $M_{V'}^2$ contains terms in addition to the pure mass term for V':

$$\frac{M_{V'}^2}{2(g_1^2 + g_2^2)} \int d^4\theta \, \mathrm{Tr}[e^{2[(g_2^2/g_1^2)\tilde{g}V' - gV]} e^{2(\tilde{g}V' + gV)}]$$

$$= \frac{1}{2} M_{V'}^2 \int d^4\theta \Big\{ V'^a V'^a - \frac{g^2}{3}[(V^a V'^a)^2 \tag{A11}$$

$$- (V^a V^a)(V'^b V'^b)]\Big\}.$$

The terms quartic in the vector multiplets are essential for maintaining the low-energy gauge invariance.[11] The equation of motion for V', to order $1/M_{V'}^2$, gives

$$V'^a = -\frac{2\tilde{g}}{M_{V'}^2} \sum_{i=u,d} H_i^\dagger \Big\{ \Big(1 - \frac{g^2}{6} V^b V^b \Big) \tau^a$$

$$+ \frac{1}{6} g V^a (3 + 2g V^a \tau^a + 2g V^b \tau^b) \Big\} H_i, \tag{A12}$$

where there is no summation over a (but there is over b), and τ^a are the $SU(2)$ generators in the fundamental representation. Replacing back in the action leads to the effective Kähler potential

$$K_{\mathrm{eff}} = H_u^\dagger e^{2gV} H_u + H_d^\dagger e^{2gV} H_d - \frac{\tilde{g}^2}{2M_{V'}^2}\{(H_u^\dagger e^{2gV} H_u$$

$$+ H_d^\dagger e^{2gV} H_d)^2 - 4|H_u \epsilon H_d|^2\}, \tag{A13}$$

where we restored the terms in V into the exponential form, and the hypercharge vector multiplet can be put back in a trivial way. Therefore, the massive W' induces the operators of Eqs. (1)–(7) with coefficients

$$c_1 = -\tilde{g}^2, \quad c_2 = -\tilde{g}^2, \quad c_3 = -\tilde{g}^2, \quad c_4 = 2\tilde{g}^2, \tag{A14}$$

$M = M_{V'}$, and all other EFT coefficients vanishing.

There are also excitations of the Σ field (a SM singlet and triplet) with masses proportional to $\langle \Sigma \rangle$. These may be split by SUSY breaking and generate further contributions to the dimension-6 operators in the effective Kähler potential. These were considered in Ref. [4] in the opposite limit that interests us here, namely, when SUSY breaking is comparable to the SUSY-preserving contribution.

For completeness, we also record here the SUSY-preserving operators induced by integrating out a massive $U(1)'$ gauge field, i.e. integrating out V' from

$$K = H_u^\dagger e^{2Q_u g'V'} H_u + H_d^\dagger e^{2Q_d g'V'} H_d + \tfrac{1}{2} M_{V'}^2 V'^2, \tag{A15}$$

where g' is the $U(1)'$ gauge coupling and $Q_{u,d}$ are the $U(1)'$ charges of $H_{u,d}$, respectively (for simplicity, we have omit-

---

ted the SM gauge factors, which are implicitly understood). Unlike in the non-Abelian case, the c_4 operator is not induced, while

$$c_1 = -4Q_d^2 g'^2, \quad c_2 = -4Q_u^2 g'^2, \quad c_3 = -4Q_u Q_d g'^2. \tag{A16}$$

From the examples above, it should be clear that MSSM extensions including singlet and triplet Higgses, plus Abelian or non-Abelian gauge factors can generate all of the operators we considered in the main text, with essentially arbitrary coefficients, except for the c_6 and c_7 operators. We have nevertheless included the latter operators in our phenomenological analysis, since they are allowed by supersymmetry.

APPENDIX B: COMMENTS ON CUSTODIAL SYMMETRY

Neglecting the Yukawa couplings, the Higgs sector in the MSSM can be written in terms of a chiral superfield

$$\Phi = \begin{pmatrix} H_d^0 & H_u^+ \\ H_d^- & H_u^0 \end{pmatrix}$$

as

$$K \supset H_u^\dagger e^{2gW + g'B} H_u + H_d^\dagger e^{2gW - g'B} H_d$$

$$= \mathrm{Tr}\Big\{ \Phi^\dagger e^{2gW} \Phi \begin{pmatrix} e^{-g'B} & 0 \\ 0 & e^{g'B} \end{pmatrix} \Big\},$$

$$W \supset \mu H_u \epsilon H_d = \frac{1}{2} \mathrm{Tr}\epsilon^T \Phi^T \epsilon \Phi,$$

where W and B are the $SU(2)_L$ and $U(1)_Y$ vector superfields, while ϵ is the antisymmetric 2-index tensor. This shows that in the limit $g' \to 0$ (and neglecting Yukawa couplings), the theory is invariant under $SU(2)_L \times SU(2)_R$ where $\Phi \to U_L \Phi U_R^\dagger$. The $SU(2)_L$ factor is gauged and can be complexified. The global $SU(2)_R$ implies that in the limit $v_u = v_d$ the theory has a custodial $SU(2)_{L+R}$ global symmetry. This symmetry has a somewhat limited use since it is broken away from $\tan\beta = 1$.

However, at tree level (and for $g' = 0$) the Higgs (scalar) sector of the MSSM exhibits an $SU(2)_L^{\mathrm{local}} \times SU(2)_R^{\mathrm{global}}$ symmetry such that the Higgs scalar components

$$\phi_u = \frac{1}{\sqrt{2}} \begin{pmatrix} H_u^{0*} & H_u^+ \\ -H_u^- & H_u^0 \end{pmatrix}, \qquad \phi_d = \frac{1}{\sqrt{2}} \begin{pmatrix} H_d^0 & -H_d^+ \\ H_d^- & H_d^{0*} \end{pmatrix},$$

transform as $\phi_{u,d} \to U_L \phi_{u,d} U_R^\dagger$. In fact, if the Higgsinos are taken to be singlets under the $SU(2)_R$ transformation, only the Higgs-Higgsino-gaugino couplings (apart from the superpotential Yukawa terms) violate this global symmetry. Thus, for arbitrary expectation values, v_u and v_d, contributions to the T parameter enter only at one loop level.

The fact that in the MSSM the tree-level gauge boson masses satisfy the SM relation $\rho = 1$ can be seen directly

---

[11]These terms are not present in the $U(1)'$ case. For instance gauging only the $U(1)_2 \subset SU(2)_2$ generated by τ^3, i.e. setting $V_2^1 = V_2^2 = 0$, the last two terms in Eq. (A11) cancel out.

from the identities $H_u^\dagger(2gW)^2 H_u = \mathrm{Tr}\Phi_u^\dagger(2gW)^2\Phi_u$ and $H_d^\dagger(2gW)^2 H_d = \mathrm{Tr}\Phi_d^\dagger(2gW)^2\Phi_d$, which lead to the gauge boson mass terms in the Kähler potential after replacing the chiral superfields by their scalar components, $\Phi_{u,d} \to \phi_{u,d}$. This observation also implies that higher-dimension operators such as $(H_u^\dagger e^{2V} H_u)(H_u\epsilon H_d + \mathrm{H.c.})$ or $(H_d^\dagger e^{2V} H_d) \times (H_u\epsilon H_d + \mathrm{H.c.})$, i.e. those in Eq. (5), lead to $\rho = 1$ at tree level. On the other hand, the higher-dimension operators of Eq. (4) contribute to the gauge boson mass terms through the linear term in $e^{2V} = 1 + 2V + \cdots$, and these terms do *not* respect a custodial symmetry. This was seen explicitly in Eq. (33). As shown above, an exception is the operator $(H_u^\dagger e^{2V} H_u + H_d^\dagger e^{2V} H_d)^2$, in the limit $v_u = v_d$. This operator is naturally induced by massive W primes, as shown in Appendix A 3.

APPENDIX C: CHARGINOS AND NEUTRALINOS

Although our focus is on the scalar Higgs sector, neutralinos and charginos can provide important decay chan-

nels, and the effects of the higher-dimension operators on their masses play an important role. We have implemented in HDECAY the corresponding mass formulas to order $1/M$, as computed in [10]. At order $1/M^2$ there are additional contributions to the mass matrix as well as to the kinetic terms that are needed to compute the physical chargino/neutralino masses. Given that these states tend to be near the experimental limits, it would be interesting to compute these next order corrections, but we postpone it to future work. For completeness, we collect the mass matrices to order $1/M$.

The chargino mass matrix is

$$(\tilde{W}^+, \tilde{H}_u^+)\begin{pmatrix} M_2 & \sqrt{2}m_W c_\beta \\ \sqrt{2}m_W s_\beta & \mu(1 - \rho s_{2\beta}) \end{pmatrix}\begin{pmatrix} \tilde{W}^- \\ \tilde{H}_d^- \end{pmatrix}, \quad \text{(C1)}$$

where $\rho \equiv \omega_1 v^2/(4\mu M)$ takes into account the effects from the heavy physics. The neutralino mass matrix is

$$\frac{1}{2}(\tilde{B}, \tilde{W}^3, \tilde{H}_d^0, \tilde{H}_u^0)\begin{pmatrix} M_1 & & -m_Z s_W c_\beta & m_Z s_W s_\beta \\ & M_2 & m_Z c_W c_\beta & -m_Z c_W s_\beta \\ -m_Z s_W c_\beta & m_Z c_W c_\beta & 2\mu\rho s_\beta^2 & -\mu(1 - 2\rho s_{2\beta}) \\ m_Z s_W s_\beta & -m_Z c_W s_\beta & -\mu(1 - 2\rho s_{2\beta}) & 2\mu\rho c_\beta^2 \end{pmatrix}\begin{pmatrix} \tilde{B} \\ \tilde{W}^3 \\ \tilde{H}_d^0 \\ \tilde{H}_u^0 \end{pmatrix}, \quad \text{(C2)}$$

where c_W stands for the weak-mixing angle $\cos\theta_W$. M_1 and M_2 are the $SU(2)_L$ and $U(1)_Y$ gaugino soft breaking parameters.

APPENDIX D: HIGGS COUPLINGS

The couplings between the Z gauge boson and two Higgs fields, defined in Eq. (40), are given by

$$\eta_{ZhA} = c_{\alpha-\beta}\{1 - \tfrac{1}{2}[(A_1 + E_1)c_\gamma - B_1 s_\gamma]\} + \tfrac{1}{2}[(D_1 + E_1)s_\gamma - B_1 c_\gamma]s_{\alpha-\beta} + c_\gamma\delta\eta_{ZhA} - s_\gamma\delta\eta_{ZHA},$$

$$\eta_{ZAh} = c_{\alpha-\beta}\{1 - \tfrac{1}{2}[(A_1 + E_1)c_\gamma - B_1 s_\gamma]\} + \tfrac{1}{2}[(D_1 + E_1)s_\gamma - B_1 c_\gamma]s_{\alpha-\beta} + c_\gamma\delta\eta_{ZAh} - s_\gamma\delta\eta_{ZAH},$$

$$\eta_{ZHA} = s_{\alpha-\beta}\{1 - \tfrac{1}{2}[(D_1 + E_1)c_\gamma + B_1 s_\gamma]\} - \tfrac{1}{2}[(A_1 + E_1)s_\gamma + B_1 c_\gamma]c_{\alpha-\beta} + c_\gamma\delta\eta_{ZHA} + s_\gamma\delta\eta_{ZhA}, \quad \text{(D1)}$$

$$\eta_{ZAH} = s_{\alpha-\beta}\{1 - \tfrac{1}{2}[(D_1 + E_1)c_\gamma + B_1 s_\gamma]\} - \tfrac{1}{2}[(A_1 + E_1)s_\gamma + B_1 c_\gamma]c_{\alpha-\beta} + c_\gamma\delta\eta_{ZAH} + s_\gamma\delta\eta_{ZAh},$$

$$\delta\eta_{ZH^+H^-} = 1 - F_1 + \delta\eta_{ZH^+H^-},$$

where γ is defined by Eq. (29), A_1, B_1, D_1, F_1, and E_1 are defined in Eq. (27), and

$$\delta\eta_{ZhA} = \frac{v^2}{M^2}s_\beta\{3t_\beta^{-1}s_\beta^2(c_2 c_\alpha + c_1 t_\beta^{-1}s_\alpha) + t_\beta^{-1}s_\beta^2[c_6(2s_\alpha - t_\beta^{-1}c_\alpha) - c_7(s_\alpha - 2t_\beta^{-1}c_\alpha)]\},$$

$$\delta\eta_{ZAh} = \frac{v^2}{M^2}s_\beta\left\{t_\beta^{-1}s_\beta^2(c_2 c_\alpha + c_1 t_\beta^{-1}s_\alpha) + \tfrac{1}{2}c_6 t_\beta^{-1}(3 - c_{2\beta})s_\alpha + \tfrac{1}{2}c_7(3 + c_{2\beta})c_\alpha\right\},$$

$$\delta\eta_{ZHA} = \frac{v^2}{M^2}s_\beta\{3t_\beta^{-1}s_\beta^2(c_2 s_\alpha - c_1 t_\beta^{-1}c_\alpha) - t_\beta^{-1}s_\beta^2[c_6(2c_\alpha + t_\beta^{-1}s_\alpha) - c_7(c_\alpha + 2t_\beta^{-1}s_\alpha)]\}, \quad \text{(D2)}$$

$$\delta\eta_{ZAH} = \frac{v^2}{M^2}s_\beta\left\{t_\beta^{-1}s_\beta^2(c_2 s_\alpha - c_1 t_\beta^{-1}c_\alpha) - \tfrac{1}{2}c_6 t_\beta^{-1}(3 - c_{2\beta})c_\alpha + \tfrac{1}{2}c_7(3 + c_{2\beta})s_\alpha\right\},$$

$$\delta\eta_{ZH^+H^-} = \frac{v^2}{M^2}s_\beta^4\left\{\tfrac{1}{4}\frac{c_W^2}{c_{2W}}c_3(1 + 3s_\beta^{-4} - 6t_\beta^{-2} + t_\beta^{-4}) + t_\beta^{-1}\left[c_6 - \frac{s_W^2}{c_{2W}}(c_1 + c_2)t_\beta^{-1} + c_7 t_\beta^{-2}\right]\right\}.$$

Similarly, the couplings between the W and the two Higgs fields, defined in Eq. (40), are given by

$$\eta_{W^\pm hH^\mp} = c_{\alpha-\beta}\{1 - \tfrac{1}{2}[(A_1 + F_1)c_\gamma - B_1 s_\gamma]\} + \tfrac{1}{2}[(D_1 + F_1)s_\gamma - B_1 c_\gamma]s_{\alpha-\beta} + c_\gamma \delta\eta_{W^\pm hH^\mp} - s_\gamma \delta\eta_{W^\pm HH^\mp},$$

$$\eta_{W^\pm H^\mp h} = c_{\alpha-\beta}\{1 - \tfrac{1}{2}[(A_1 + F_1)c_\gamma - B_1 s_\gamma]\} + \tfrac{1}{2}[(D_1 + F_1)s_\gamma - B_1 c_\gamma]s_{\alpha-\beta} + c_\gamma \delta\eta_{W^\pm H^\mp h} - s_\gamma \delta\eta_{W^\pm H^\mp H},$$

$$\eta_{W^\pm HH^\mp} = s_{\alpha-\beta}\{1 - \tfrac{1}{2}[(D_1 + F_1)c_\gamma + B_1 s_\gamma]\} - \tfrac{1}{2}[(A_1 + F_1)s_\gamma + B_1 c_\gamma]c_{\alpha-\beta} + c_\gamma \delta\eta_{W^\pm HH^\mp} + s_\gamma \delta\eta_{W^\pm hH^\mp}, \quad \text{(D3)}$$

$$\eta_{W^\pm H^\mp H} = s_{\alpha-\beta}\{1 - \tfrac{1}{2}[(D_1 + F_1)c_\gamma + B_1 s_\gamma]\} - \tfrac{1}{2}[(A_1 + F_1)s_\gamma + B_1 c_\gamma]c_{\alpha-\beta} + c_\gamma \delta\eta_{W^\pm H^\mp H} + s_\gamma \delta\eta_{W^\pm H^\mp h},$$

$$\eta_{W^\pm H^\mp A} = 1 - \tfrac{1}{2}(E_1 + F_1) + \delta\eta_{W^\pm H^\mp A}, \qquad \eta_{W^\pm AH^\mp} = 1 - \tfrac{1}{2}(E_1 + F_1) + \delta\eta_{W^\pm AH^\mp},$$

where

$$\delta\eta_{W^\pm hH^\mp} = \frac{v^2}{M^2} s_\beta^3 \left\{ \frac{1}{8} c_3[(3 + s_\beta^{-2} - 9t_\beta^{-1})s_\alpha - (t_\beta^{-1}(9 - s_\beta^{-2}) - 3t_\beta^{-3})c_\alpha] + \frac{3}{2} t_\beta^{-1}(c_1 t_\beta^{-1} s_\alpha + c_2 c_\alpha) \right\},$$

$$\delta\eta_{W^\pm H^\mp h} = \frac{v^2}{2M^2} s_\beta^3 \{ c_3(s_\alpha + t_\beta^{-3} c_\alpha) + t_\beta^{-1}(c_1 t_\beta^{-1} s_\alpha + c_2 c_\alpha) \},$$

$$\delta\eta_{W^\pm HH^\mp} = \frac{v^2}{2M^2} s_\beta^3 \left\{ \frac{1}{4} c_3[(3 + s_\beta^{-2} - 9t_\beta^{-2})c_\alpha + (t_\beta^{-1}(9 - s_\beta^{-2}) - 3t_\beta^{-3})s_\alpha] + 3t_\beta^{-1}(c_1 t_\beta^{-1} c_\alpha - c_2 s_\alpha) \right\},$$

$$\delta\eta_{W^\pm H^\mp H} = \frac{v^2}{2M^2} s_\beta^3 \{ c_3(c_\alpha - t_\beta^{-3} s_\alpha) + t_\beta^{-1}(c_1 t_\beta^{-1} c_\alpha - c_2 s_\alpha) \},$$

$$\delta\eta_{W^\pm H^\mp A} = \frac{v^2}{2M^2} s_\beta^4 \left\{ 3(c_1 + c_2)t_\beta^{-2} - \frac{1}{4} c_3(1 - 5s_\beta^{-4} - 6t_\beta^{-2} + t_\beta^{-4}) \right\},$$

$$\delta\eta_{W^\pm AH^\mp} = \frac{v^2}{8M^2} s_\beta^4 \{ 4t_\beta^{-2}(c_1 + c_2) + c_3(1 + 3s_\beta^{-4} - 6t_\beta^{-2} + t_\beta^{-4}) \}.$$

(D4)

[1] J. F. Gunion and H. E. Haber, Nucl. Phys. **B272**, 1 (1986); **B402**, 567(E) (1993).

[2] Y. Okada, M. Yamaguchi, and T. Yanagida, Prog. Theor. Phys. **85**, 1 (1991); J. R. Ellis, G. Ridolfi, and F. Zwirner, Phys. Lett. B **257**, 83 (1991); S. P. Li and M. Sher, Phys. Lett. **140B**, 339 (1984); R. Barbieri and M. Frigeni, Phys. Lett. B **258**, 395 (1991); M. Drees and M. M. Nojiri, Phys. Rev. D **45**, 2482 (1992); J. A. Casas, J. R. Espinosa, M. Quirós, and A. Riotto, Nucl. Phys. **B436**, 3 (1995); **B439**, 466(E) (1995); J. R. Ellis, G. Ridolfi, and F. Zwirner, Phys. Lett. B **262**, 477 (1991); A. Brignole, J. R. Ellis, G. Ridolfi, and F. Zwirner, Phys. Lett. B **271**, 123 (1991); R. Barbieri, M. Frigeni, and F. Caravaglios, Phys. Lett. B **258**, 167 (1991); H. E. Haber and R. Hempfling, Phys. Rev. Lett. **66**, 1815 (1991); M. S. Carena, M. Quirós, and C. E. M. Wagner, Nucl. Phys. **B461**, 407 (1996).

[3] J. R. Espinosa and M. Quirós, Phys. Rev. Lett. **81**, 516 (1998).

[4] P. Batra, A. Delgado, D. E. Kaplan, and T. M. P. Tait, J. High Energy Phys. 02 (2004) 043; R. Harnik, G. D. Kribs, D. T. Larson, and H. Murayama, Phys. Rev. D **70**, 015002 (2004); P. Batra, A. Delgado, D. E. Kaplan, and T. M. P. Tait, J. High Energy Phys. 06 (2004) 032; A. Birkedal, Z. Chacko, and Y. Nomura, Phys. Rev. D **71**, 015006 (2005).

[5] R. Dermisek and J. F. Gunion, Phys. Rev. Lett. **95**, 041801 (2005); S. Chang, P. J. Fox, and N. Weiner, J. High Energy Phys. 08 (2006) 068; L. M. Carpenter, D. E. Kaplan, and E. J. Rhee, Phys. Rev. Lett. **99**, 211801 (2007).

[6] M. Dine, N. Seiberg, and S. Thomas, Phys. Rev. D **76**, 095004 (2007).

[7] K. S. Babu, I. Gogoladze, M. U. Rehman, and Q. Shafi, Phys. Rev. D **78**, 055017 (2008).

[8] A. Brignole, J. A. Casas, J. R. Espinosa, and I. Navarro, Nucl. Phys. **B666**, 105 (2003).

[9] H. E. Haber and R. Hempfling, Phys. Rev. D **48**, 4280 (1993); J. F. Gunion and H. E. Haber, Phys. Rev. D **67**, 075019 (2003).

[10] P. Batra and E. Pontón, Phys. Rev. D **79**, 035001 (2009).

[11] P. Fayet, Nucl. Phys. **B90**, 104 (1975); R. K. Kaul and P. Majumdar, Nucl. Phys. **B199**, 36 (1982).

[12] H. E. Haber and G. L. Kane, Phys. Rep. **117**, 75 (1985).

[13] R. Harnik, G. D. Kribs, D. T. Larson, and H. Murayama, Phys. Rev. D **70**, 015002 (2004); S. Chang, C. Kilic, and R. Mahbubani, Phys. Rev. D **71**, 015003 (2005); A. Delgado and T. M. P. Tait, J. High Energy Phys. 07 (2005) 023.

[14] M. Carena, K. Kong, E. Pontón, and J. Zurita (unpublished).

[15] A. Strumia, Phys. Lett. B **466**, 107 (1999).

[16] I. Antoniadis, E. Dudas, and D. M. Ghilencea, J. High Energy Phys. 03 (2008) 045; I. Antoniadis, E. Dudas, D. M. Ghilencea, and P. Tziveloglou, Nucl. Phys. **B808**, 155 (2009); I. Antoniadis, E. Dudas, D. M. Ghilencea, and P. Tziveloglou, AIP Conf. Proc. **1078**, 175 (2009).

[17] K. Blum, C. Delaunay, and Y. Hochberg, Phys. Rev. D **80**, 075004 (2009).

[18] J. A. Casas, J. R. Espinosa, and I. Hidalgo, J. High Energy Phys. 01 (2004) 008.

[19] S. Cassel, D. M. Ghilencea, and G. G. Ross, Nucl. Phys. **B825**, 203 (2010).

[20] K. Cheung, S. Y. Choi, and J. Song, Phys. Lett. B **677**, 54 (2009).

[21] M. Berg, J. Edsjo, P. Gondolo, E. Lundstrom, and S. Sjors, J. Cosmol. Astropart. Phys. 08 (2009) 035.

[22] N. Bernal, K. Blum, M. Losada, and Y. Nir, J. High Energy Phys. 08 (2009) 053.

[23] C. Grojean, G. Servant, and J. D. Wells, Phys. Rev. D **71**, 036001 (2005).

[24] D. Bodeker, L. Fromme, S. J. Huber, and M. Seniuch, J. High Energy Phys. 02 (2005) 026.

[25] C. Delaunay, C. Grojean, and J. D. Wells, J. High Energy Phys. 04 (2008) 029.

[26] A. Noble and M. Perelstein, Phys. Rev. D **78**, 063518 (2008).

[27] B. Grinstein and M. Trott, Phys. Rev. D **78**, 075022 (2008).

[28] A. D. Medina, N. R. Shah, and C. E. M. Wagner, Phys. Rev. D **80**, 015001 (2009).

[29] M. E. Peskin and T. Takeuchi, Phys. Rev. Lett. **65**, 964 (1990); Phys. Rev. D **46**, 381 (1992).

[30] S. Di Chiara and K. Hsieh, Phys. Rev. D **78**, 055016 (2008).

[31] T. Inami, C. S. Lim, and A. Yamada, Mod. Phys. Lett. A **7**, 2789 (1992).

[32] D. Choudhury, T. M. P. Tait, and C. E. M. Wagner, Phys. Rev. D **65**, 115007 (2002).

[33] Z. Han and W. Skiba, Phys. Rev. D **71**, 075009 (2005); Z. Han, Phys. Rev. D **73**, 015005 (2006).

[34] Tevatron Electroweak Working Group, CDF Collaboration, and D0 Collaboration, arXiv:0903.2503.

[35] CDF Collaboration and D0 Collaboration, arXiv:0808.0147.

[36] A. Djouadi, J. Kalinowski, and M. Spira, Comput. Phys. Commun. **108**, 56 (1998).

[37] M. S. Carena, J. R. Espinosa, M. Quirós, and C. E. M. Wagner, Phys. Lett. B **355**, 209 (1995).

[38] M. S. Carena, M. Olechowski, S. Pokorski, and C. E. M. Wagner, Nucl. Phys. **B426**, 269 (1994); D. M. Pierce, J. A. Bagger, K. T. Matchev, and R. j. Zhang, Nucl. Phys. **B491**, 3 (1997); M. S. Carena, D. Garcia, U. Nierste, and C. E. M. Wagner, Nucl. Phys. **B577**, 88 (2000).

[39] S. Dawson, A. Djouadi, and M. Spira, Phys. Rev. Lett. **77**, 16 (1996).

[40] A. Menon and D. E. Morrissey, Phys. Rev. D **79**, 115020 (2009).

[41] H. M. Georgi, S. L. Glashow, M. E. Machacek, and D. V. Nanopoulos, Phys. Rev. Lett. **40**, 692 (1978).

[42] M. Spira, A. Djouadi, D. Graudenz, and P. M. Zerwas, Nucl. Phys. **B453**, 17 (1995).

[43] S. Mantry, M. Trott, and M. B. Wise, Phys. Rev. D **77**, 013006 (2008).

[44] L. Randall, J. High Energy Phys. 02 (2008) 084.